Human Reproduction, Vol.31, No.1 pp. 133–149, 2016
Advanced Access publication on November 17, 2015 doi:10.1093/humrep/dev279

human reproduction

ORIGINAL ARTICLE ***Reproductive biology***

Postovulatory aging affects dynamics of mRNA, expression and localization of maternal effect proteins, spindle integrity and pericentromeric proteins in mouse oocytes

T. Trapphoff[1], M. Heiligentag[1], D. Dankert[2], H. Demond[3], D. Deutsch[4], T. Fröhlich[4], G.J. Arnold[4], R. Grümmer[2], B. Horsthemke[3], and U. Eichenlaub-Ritter[1,*]

[1]Institute of Gene Technology/Microbiology, University of Bielefeld, Bielefeld, Germany [2]Institute of Anatomy, University Hospital, University Duisburg-Essen, Essen, Germany [3]Institute of Human Genetics, University Hospital, University Duisburg-Essen, Essen, Germany [4]Laboratory for Functional Genome Analysis, Gene Center, Ludwig-Maximilians-Universität München, Munich, Germany

*Correspondence address. Institute of Gene Technology/Microbiology, University of Bielefeld, Bielefeld, Germany. E-mail: eiri@uni-bielefeld.de

Submitted on July 27, 2015; resubmitted on October 6, 2015; accepted on October 13, 2015

STUDY QUESTION: Is the postovulatory aging-dependent differential decrease of mRNAs and polyadenylation of mRNAs coded by maternal effect genes associated with altered abundance and distribution of maternal effect and RNA-binding proteins (MSY2)?

SUMMARY ANSWER: Postovulatory aging results in differential reduction in abundance of maternal effect proteins, loss of RNA-binding proteins from specific cytoplasmic domains and critical alterations of pericentromeric proteins without globally affecting protein abundance.

WHAT IS KNOWN ALREADY: Oocyte postovulatory aging is associated with differential alteration in polyadenylation and reduction in abundance of mRNAs coded by selected maternal effect genes. RNA-binding and -processing proteins are involved in storage, polyadenylation and degradation of mRNAs thus regulating stage-specific recruitment of maternal mRNAs, while chromosomal proteins that are stage-specifically expressed at pericentromeres, contribute to control of chromosome segregation and regulation of gene expression in the zygote.

STUDY DESIGN, SIZE, DURATION: Germinal vesicle (GV) and metaphase II (MII) oocytes from sexually mature C57Bl/6J female mice were investigated. Denuded *in vivo or in vitro* matured MII oocytes were postovulatory aged and analyzed by semiquantitative confocal microscopy for abundance and localization of polyadenylated RNAs, proteins of maternal effect genes (transcription activator BRG1 also known as ATP-dependent helicase SWI/SNF related, matrix associated, actin dependent regulator of chromatin, subfamily a, member 4 (SMARCA4) and NOD-like receptor family pyrin domain containing 5 (NLRP5) also known as MATER), RNA-binding proteins (MSY2 also known as germ cell-specific Y-box-binding protein, YBX2), and post-transcriptionally modified histones (trimethylated histone H3K9 and acetylated histone H4K12), as well as pericentromeric ATRX (alpha thalassemia/mental retardation syndrome X-linked, also termed ATP-dependent helicase ATRX or X-linked nuclear protein (XNP)). For proteome analysis five replicates of 30 mouse oocytes were analyzed by selected reaction monitoring (SRM).

MATERIAL AND METHODS: GV and MII oocytes were obtained from large antral follicles or ampullae of sexually mature mice, respectively. Denuded MII oocytes were aged for 24 h post ovulation. For analysis of distribution and abundance of polyadenylated RNAs fixed oocytes were *in situ* hybridized to Cy5 labeled oligo$(dT)_{20}$ nucleotides. Absolute quantification of protein concentration per oocyte of selected proteins was done by SRM proteome analysis. Relative abundance of ATRX was assessed by confocal laser scanning microscopy (CLSM) of whole mount formaldehyde fixed oocytes or after removal of zona and spreading. MSY2 protein distribution and abundance was studied in MII oocytes prior to, during and after exposure to nocodazole, or after aging for 2 h in presence of H_2O_2 or for 24 h in presence of a glutathione donor, glutathione ethylester (GEE).

MAIN RESULTS AND ROLE OF CHANCE: The significant reduction in abundance of proteins ($P < 0.001$) translated from maternal mRNAs was independent of polyadenylation status, while their protein localization was not significantly changed by aging. Most of other proteins

quantified by SRM analysis did not significantly change in abundance upon aging except MSY2 and GTSF1. MSY2 was enriched in the subcortical RNP domain (SCRD) and in the spindle chromosome complex (SCC) in a distinct pattern, right and left to the chromosomes. There was a significant loss of MSY2 from the SCRD ($P < 0.001$) and the spindle after postovulatory aging. Microtubule de- and repolymerization caused reversible loss of MSY2 spindle-association whereas H_2O_2 stress did not significantly decrease MSY2 abundance. Aging in presence of GEE decreased significantly ($P < 0.05$) the aging-related overall and cytoplasmic loss of MSY2. Postovulatory aging increased significantly spindle abnormalities, unaligned chromosomes, and abundance of acetylated histone H4K12, and decreased pericentromeric trimethylated histone H3K9 (all $P < 0.001$). Spreading revealed a highly significant increase in pericentromeric ATRX ($P < 0.001$) upon ageing. Thus, the significantly reduced abundance of MSY2 protein, especially at the SCRD and the spindle may disturb the spatial control and timely recruitment, deadenylation and degradation of developmentally important RNAs. An autonomous program of degradation appears to exist which transiently and specifically induces the loss and displacement of transcripts and specific maternal proteins independent of fertilization in aging oocytes and thereby can critically affect chromosome segregation and gene expression in the embryo after fertilization.

LIMITATION, REASONS FOR CAUTION: We used the mouse oocyte to study processes associated with postovulatory aging, which may not entirely reflect processes in aging human oocytes. However, increases in spindle abnormalities, unaligned chromosomes and H4K12 acetylated histones, as well as in mRNA abundance and polyadenylation have been observed also in aged human oocytes suggesting conserved processes in aging.

WIDER IMPLICATIONS OF THE FINDINGS: Postovulatory aging precociously induces alterations in expression and epigenetic modifications of chromatin by ATRX and in histone pattern in MII oocytes that normally occur after fertilization, possibly contributing to disturbances in the oocyte-to-embryo transition (OET) and the zygotic gene activation (ZGA). These observations in mouse oocytes are also relevant to explain disturbances and reduced developmental potential of aged human oocytes and caution to prevent oocyte aging *in vivo* and *in vitro*.

STUDY FUNDING/COMPETING INTERESTS: The study has been supported by the German Research Foundation (DFG) (EI 199/7-1 | GR 1138/12-1 | HO 949/21-1 and FOR 1041). There is no competing interest.

Key words: oocyte / aging / gene expression / RNA dynamics / maternal effect genes / centromere / spindle chromosome complex / histone pattern

Introduction

Numerous studies show that postovulatory aging leads to limited oocyte competence, abnormal development, congenital malformations and reduced pregnancy outcomes in various laboratory animals (Blandau and Young, 1939; Chang, 1952; Kosubek *et al.*, 2010). However, the molecular mechanisms leading to altered intracellular homeostasis, still remain largely unknown. Involvement of oxidative stress, mitochondrial dysfunction or differences in expression have been postulated (e.g. Lacham-Kaplan and Trounson, 2008; Miao *et al.*, 2009; Tatone *et al.*, 2011; Zhang *et al.*, 2011; Lord *et al.*, 2013; Takahashi *et al.*, 2013; Cecconi *et al.*, 2014). Delayed fertilization has a detrimental effect on the mRNA content and the poly(A)-tail length of selected maternal effect genes including *Nlrp5* (NLR family, pyrin domain containing 5; also known as MATER), and *Brg1* (SWI/SNF related, matrix associated, actin dependent regulator of chromatin) an ATP-dependent helicase encoded by the *SMARCA4* gene in human (Dankert *et al.*, 2014). Whether this also affects protein processing and synthesis, and thus ultimately contributes to functional or developmental defects is unknown.

Maternal effect genes (MEGs) affecting the phenotype in the early embryo (Kim and Lee, 2014; Zhang and Smith, 2015) are mandatory for the oocyte to embryo transition (OET), to ensure genomic reprogramming and embryonic totipotency, recruitment and degradation of maternal mRNAs and proteins, and establishment and protection of epigenetic histone and DNA modifications (Bultman *et al.*, 2006; Su *et al.*, 2007; Messerschmidt *et al.*, 2012). Disruption of MEGs results in defective early embryogenesis. During oocyte growth, some MEGs (and other maternal factors) become accumulated at the protein and transcript level in specific subcellular compartments (Li *et al.*, 2008; Flemr *et al.*, 2010).

In transcriptionally quiescent maturing oocytes and early embryos, stored maternal factors like mRNAs and proteins become recruited, modified and expressed in a stage-specific and timed manner to ensure normal OET and zygotic gene activation (ZGA) (Bettegowda and Smith, 2007; Fair, 2010; Li *et al.*, 2010; Zuccotti *et al.*, 2011; Clift and Schuh, 2013; Norbury, 2013; Ma *et al.*, 2015). Long-term storage of mRNAs during oocyte growth requires mRNA-binding proteins like the intracellular germ cell-specific mRNA binding protein MSY2 (also termed YBX2, Y-box-binding protein 2 in human, and FRGY2 in *Xenopus*), a conserved protein that confers stability to mRNAs as well as translational repression (Medvedev *et al.*, 2011; Ma *et al.*, 2015).

Preimplantation development relies also on epigenetic histone and DNA modifications, and disturbances in expression are relevant for genomic integrity (Yan *et al.*, 2013). Increases in H4K12 acetylation have been implicated in susceptibility to maternal-age related meiotic errors in human oocytes (Van den Berg *et al.*, 2011). Histone H3K9 deacetylation on maternal chromatin is followed by its trimethylation during oogenesis (Peters *et al.*, 2001; Grewal and Jia, 2007). Subsequent recruitment of heterochromatin protein 1, alpha thalassemia/mental retardation syndrome X-linked (ATRX) chromatin remodeling factor and Aurora Kinases is a crucial process after resumption of meiosis I to form a bipolar spindle (Muramatsu *et al.*, 2013; Trapphoff *et al.*, 2013; Sidler *et al.*, 2014).

We showed recently that aging of *Xenopus tropicalis* and *Mus musculus* oocytes leads to the degradation of maternal mRNAs (Kosubek *et al.*, 2010; Dankert *et al.*, 2014). Moreover, postovulatory aging of mouse oocytes resulted in deadenylation and degradation of *Nlrp5* mRNA, while the level of *Brg1* mRNA was decreased without affecting poly(A)-tail characteristics (Dankert *et al.*, 2014). Therefore, we now investigated

the downstream effects at the protein level, and also identified additional factors involved in the age-dependent transcriptome alterations by semi-quantitative confocal laser scanning microscopy (CLSM), western blot and absolute protein quantification by novel selected reaction monitoring (SRM) proteomics (Fröhlich and Arnold, 2011; Deutsch *et al.*, 2014). Concomitantly, spindle formation, chromosome alignment, histone H3K9 trimethylation and histone H4K12 acetylation, as well as recruitment and relative abundance of ATRX was studied to assess functional consequences of aging that may also be critical for human oocytes and affect developmental potential and health of offspring.

Materials and Methods

Postovulatory aging of *in vivo*-grown oocytes

C57Bl/6J female mice were housed under standard conditions (12 h dark and 12 h light cycle, food and water ad libitum) in the university animal facilities in Bielefeld or Essen. Germinal vesicle oocytes (GV) were obtained from the ovaries after puncture of large antral follicles. For postovulatory aging, cumulus oocyte complexes (COCs) of *in vivo*-grown and ovulated MII oocytes (IVO) were collected from hormonally primed mice 14 h after hCG (Dankert *et al.*, 2014). Cumulus was removed by hyaluronidase (2 min at 37°C) and denuded MII oocytes were either processed immediately or postovulatory-aged for 24 h in M2 medium in a CO_2-gassed incubator at 37°C before freezing at −80°C, or immunostaining. MII oocytes were exposed to 10 mM H_2O_2 (2 h) or 1 mM glutathione ethylester (GEE) (24 h). Spindle de- and repolymerization was achieved by exposure to 10 μg/ml nocodazole for 10, 30 or 60 min.

Spindle analysis, semi-quantitative protein assessment by confocal microscopy, and *in situ* hybridization to study abundance and distribution of protein and poly(A)-mRNA

Denuded oocytes were fixed, permeabilized and blocked as previously described (see Trapphoff *et al.*, 2010, 2013; Demant *et al.*, 2012). Assessment of polyadenylated mRNAs was performed by *in situ* hybridization with single strand 5′-Cy5-oligonucleotide$(dT)_{20}$ probe (Sigma) in fixed oocytes (4% w/v PFA, 60 min at room temperature (RT); permeabilization in 0.1% Triton X-100 for 15 min at RT, hybridization with 1 μM single strand 5′-Cy5-oligonukleotide$(dT)_{20}$ probe for 1 h at 42°C, followed by 0.1% w/v BSA, 0.01% w/v Tween-20, 60′ at RT). Distribution and abundance of NLRP5, MSY2, BRG1, trimethylated H3K9, acetylated H4K12, ATRX and spindle analysis, was assessed by immunofluorescence with the following first antibodies: rabbit polyclonal anti-BRG1, rabbit polyclonal anti-NLRP5, rabbit polyclonal anti-ATRX, or goat polyclonal anti-MSY2 (all Santa Cruz, USA), monoclonal mouse anti-α-tubulin antibody (Sigma), or rabbit polyclonal anti-trimethylated H3K9 and rabbit anti-acetylated H4K12 (both Epigentek). This was followed by reaction with specific fluorescent-labeled secondary antibodies. Chromosomes were stained by Sytox Green dye (Invitrogen) or 4,6-diamindino-2-phenylindole (DAPI). Whole mount fixation of oocytes was either in 4% PFA for 30 min at 4°C, permeabilization by 0.5% w/v Triton X-100, 15 min at RT, and blocking by 0.1% w/v BSA and 0.1% w/v Tween-20 for 60 min at 37°C or after Zona pellucida removal by pronase treatment, fixation in 4% w/v PFA at 60 min at 4°C, permeabilization by 0.5% Triton X-100 for 30 min at RT, and blocking by 0.2% w/v sodium azide, 2% v/v normal goat serum, 0.2% w/v powdered milk, 0.1 M v/v glycine, 0.01% v/v Triton X-100, 1% w/v BSA for 30 min at RT. For spindle analysis oocytes were fixed by 2% w/v PFA, 0.1% v/v Triton X-100, 1 μM taxol, 0.01% w/v aprotinine, 5 mM $MgCl_2$ and 2.5 mM EGTA for 45 min at 37°C, followed by blocking by 0.2% w/v sodium azide, 2% v/v normal goat serum, 0.2% w/v powdered milk, 0.1 M v/v glycine, 0.01% v/v Triton X-100, and 1% w/v BSA for 60 min at 37°C.

Semi-quantitative protein abundance of BRG1, NLRP5 and MSY2 was determined by assessing mean fluorescence intensity [arbitrary units (a.u.) ± SE] by Leica LCSSP2 CLSM and Leica Lite software. Quantification was performed in optical sections as previously described (Demant *et al.*, 2012). Spindle morphology, chromosome alignment and ATRX pattern were analyzed by z-axial scanning with sequential scan mode using Leica LCSSP2 CLSM.

Whole mount fixed oocytes were classified as 'ATRX-strong' when the mean signal intensity was above 30 arbitrary units [a.u.; intensity range 0–255] per chromosome set; otherwise as 'ATRX-low'. For spreading, the Zona pellucida was removed followed by gentle spreading (Hodges and Hunt, 2002; Vogt *et al.*, 2010; Chambon *et al.*, 2013). Images of trimethylated H3K9 and acetylated H4K12 were recorded by Zeiss Axiophot fluorescence microscope with set exposure time. Fluorescence intensity was quantified as mean value in arbitrary units [a.u. ± SE] with ImageJ software (Trapphoff *et al.*, 2013).

RNA isolation and qRT–PCR analysis of Msy2 transcript abundance

Total RNA was obtained from 3 pools of 20 oocytes for control and aged oocytes and processed as described previously (Dankert *et al.*, 2014). Relative quantification of gene expression was determined in comparison to controls using a standard curve of Luciferase control RNA (Promega).

MSY2 western blot analysis

Protein extracts from lysed, homogenized, and boiled supernatants of 150 oocytes/experimental group were separated by electrophoresis in 17.5% SDS polyacrylamide gels, blotted to an Optidran BA-S85 nitrocellulose membrane (Whatman) and reacted with goat anti-MSY2 polyclonal antibody overnight at 4°C. After washing, membranes were reacted with biotinylated anti-goat secondary antibodies for 3 h at RT, followed by incubation in alkaline phosphatase (AP) conjugated to streptavidin for 80 min at RT. AP activity was determined using NBT/BCIP solution according to manufacturer's protocol (Roche). Lane signal intensity was quantified as relative area under curve in arbitrary units [a.u.] using ImageJ software.

Selected reaction monitoring

Selected proteins (MSY2, PDCD5, RPS27A, UHRF1, SMARCC1, STMN1 and GTSF; Table I) were quantified in five biological replicates in batches containing 30 oocytes in control and postovulatory aged groups by an absolute or relative quantification SRM approach.

For further details of SRM analysis, see Supplementary data.

Statistics

Jarque–Bera pre-test was employed to assess non-parametric or parametric characteristics of each sample cohort. Non-parametric Mann–Whitney *U*-test post-test was used for analysis of H3K9 trimethylation and H4K12 acetylation, quantity of poly(A)-mRNA, and semi-quantitative protein abundance of BRG1, NLRP5 and MSY2. ATRX-pattern, spindle integrity and chromosome alignment was analyzed using χ^2 test. GraphPad Prism 6.04 (GraphPad Software) was used for graphical illustration and statistical analysis of SRM data (multiple *t*-tests). Differences were regarded as significant in case of $P < 0.05$ and $\log_2$ fold change $\geq |0.6|$.

Table I Proteins for which selected reaction monitoring (SRM) assays were established.

Protein name	Gene name	Peptide sequences	SI peptide[a]
E3 ubiquitin-protein ligase UHRF1	*Uhrf1*	YAPAEGNR LNDTIQLLVR	A
Y-box-binding protein	*Msy2*	TPGNQATAASGTPAPPAR GAEAANVTGPGGVPVK	A
Programmed cell death protein 5	*Pdcd5*	VSEQGLIEILEK NSILAQVLDQSAR	B
Ubiquitin-40S ribosomal protein S27a	*Rps27A*	ESTLHLVLR TLSDYNIQK	B
Gametocyte specific factor 1	*Gtsf1*	LATCPFNAR SCIEQDVVNQTR	C
Stathmin	*Stmn1*	ASGQAFELILSPR AIEENNNFSK	C
SWI/SNF complex subunit SMARCC1	*Smarcc1*	EKPIDLQNFGLR AALEEFSR	C

[a]A: SpikeTides TQL peptides (JPT Peptide Technologies GmbH, Berlin), B: HeavyPeptide AQUA™ Ultimate peptides (Thermo Fisher, Rockford, IL, USA), C: Crude PEPotecSRM peptides (Thermo Fisher, Rockford, IL, USA).

Results

Abundance of polyadenylated mRNAs becomes reduced by aging

In situ hybridization of poly(dT)$_{20}$-oligonucleotides revealed a prominent accumulation of poly(A)-mRNAs in the nucleus of GV controls (Fig. 1A). Poly(A)-mRNAs were heterogeneously distributed within the cytoplasm and in distinct cytoplasmic clusters at MII stage (Fig. 1A′), predominately in the more centrally located cytoplasmic regions and less in the outer subcortical area. After postovulatory aging, MII polyadenylated mRNAs were significantly reduced in the entire ooplasm as compared with MII controls (Fig. 1A″, A‴; $P < 0.001$).

BRG1 abundance is reduced by aging while localization is not affected

The maternal effect protein BRG1 (SMARCA4) was mainly localized in the perinuclear area and in the nucleus of control GV oocytes (red labeling in Fig. 1B). At MII stage, BRG1 was in the cytosol with some prominent foci in the more peripheral region of the ooplasm but not within an area close to chromosomes and spindle (arrowhead, Fig. 1B′). After postovulatory aging the relative protein abundance was significantly decreased compared with controls (Fig. 1 B″, B‴; $P < 0.001$) while overall distribution was comparable to controls (Fig. 1B″).

NLRP5 is enriched in the subcortical maternal complex and becomes reduced by aging

NLRP5 (MATER) protein, was present in the entire ooplasm of GV controls (Fig. 1C), and appeared highly enriched in the subcortical region beneath the oolemma at MII stage (Fig. 1C′), representing the SCMC (Li *et al.*, 2008; Ohsugi *et al.*, 2008). NLRP5 enrichment in the SCMC and also in the cytoplasm was significantly decreased after postovulatory aging (Fig. 1C″, C‴; $P < 0.001$).

mRNA binding factor MSY2 is enriched in cortex and spindle and particularly lost from these domains after aging

CLSM analysis of MSY2, an essential mRNA binding factor (Medvedev *et al.*, 2008, 2011; Flemr *et al.*, 2010; Ma *et al.*, 2013, 2015) revealed an accumulation of MSY2 in the subcortical RNA domain (SCRD) and in the cytosol of GV stage oocytes, while MSY2 protein was less prominent in the nucleus (GV, Fig. 2A). At prometaphase of meiosis I, MSY2 was mainly accumulated in the subcortex and homogeneously distributed in the cytosol and not in the spindle chromosome complex (SCC) (Fig. 2B). In contrast, MSY2 was enriched in the midzone of the spindle, right and left to the cytokinesis furrow and between the segregating chromosomes at first telophase (arrowhead in Fig. 2C). At MII MSY2 was enriched in the subcortical RNA domain (arrowhead in Fig. 2D) and also in the spindle chromosome complex (arrowhead in Fig. 2D) to the left and right side of the equatorial plane within the spindle halves. It was not present on interpolar microtubules, in the central part of the spindle occupied by the chromosomes (Fig. 2D′, J, J′; arrow), or at the anastral spindle poles (Fig. 2D, J, J′).

Postovulatory aging resulted in loss of MSY2 in the SCC domain (Fig. 2E, E′) and in a translocation from the subcortical region to the cytoplasm (Fig. 2E). The *x*-axis profile of the relative MSY2 mean abundance assessed as intensity of antibody staining through a cross-section of the entire cell (white stippled line in Fig. 2F) revealed the enrichment of protein in the cortex (blue line in Fig. 2G). Scanning through the center of aged oocytes demonstrated the loss of staining from cortical regions (red line in Fig. 2G). By analysis of the relative staining intensity of the overall ooplasm (indicated by the green circle surrounding the oocyte in Fig. 2F), or the subcortical and the inner cytoplasmic regions separately (subtracting background staining in regions of interests outside of the oocyte; ROI$_3$) revealed the prominent and significant loss of overall and especially of cortical MSY2, and a relatively slight but significant increase in cytoplasmic localization (Fig. 2H). 3D analysis of

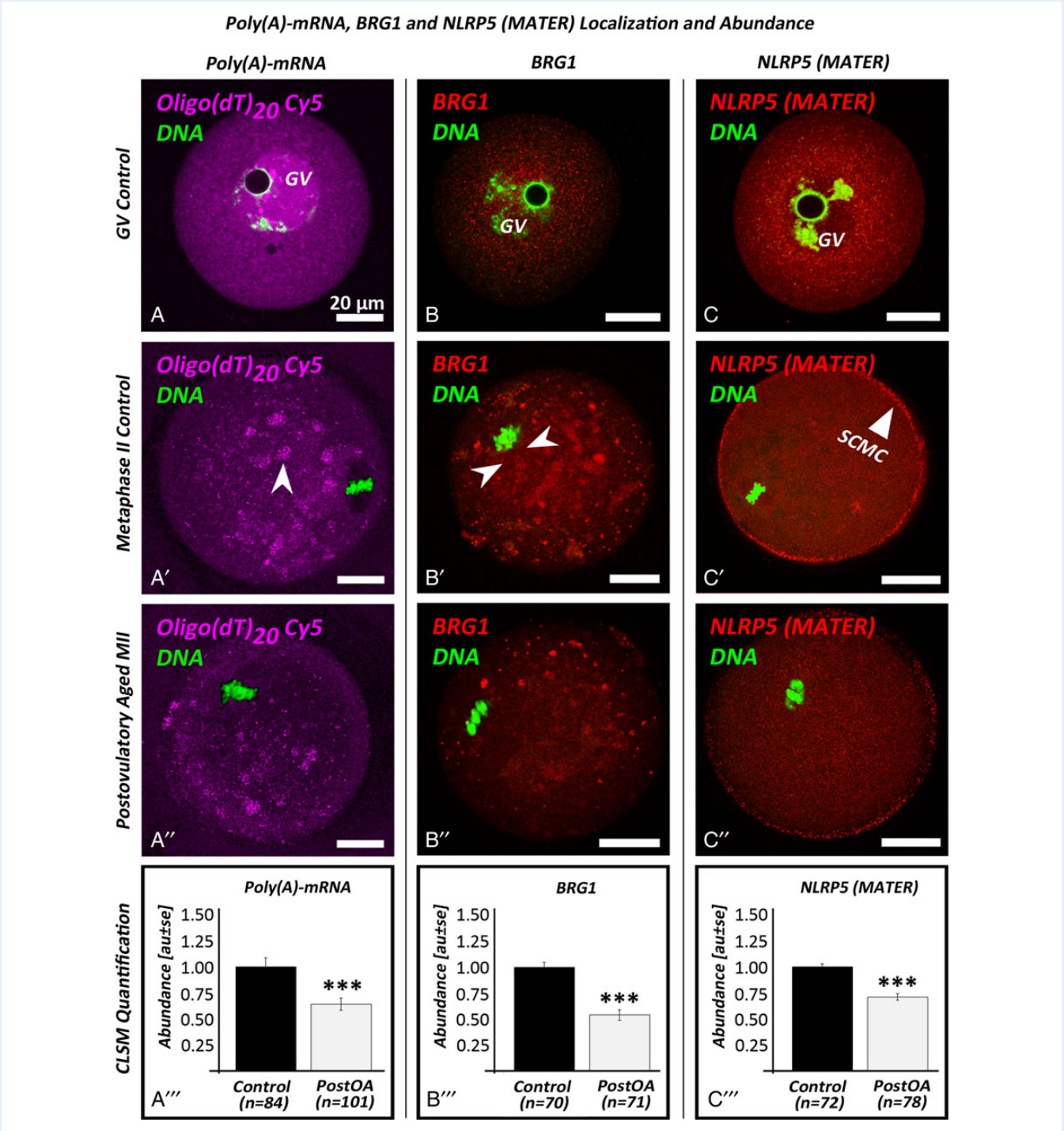

Figure 1 Localization and abundance of polyadenylated mRNA (**A**–**A‴**), and BRG1 (**B**–**B‴**) and NLRP5 protein (**C**–**C‴**). Poly(A)-mRNA in the nucleus of the germinal vesicle (GV) but not in the nucleolus of a maturation competent oocyte (A); cytoplasmic distribution and enrichment of Poly(A) transcripts in distinct clusters outside of the spindle in metaphase II (MII) controls (A′); reduced signal for Poly(A) transcripts in cytoplasm of postovulatory-aged MII oocytes (A″); relative abundance of poly(A)-mRNA as assessed by semi-quantitative analysis of confocal laser scanning microscopy (CLSM) images by ImageJ (A‴). Mainly perinuclear and nuclear, and only faint cytoplasmic immunofluorescent staining for BRG1 in GV oocytes (B); disperse and clustered (arrow) cytosolic distribution of BRG1 with no foci of BRG1 in the vicinity of the spindle (arrow) of the MII control oocyte (B′); reduced staining for BRG1 with some cytoplasmic foci in a postovulatory-aged MII oocyte (B″); relative abundance of BRG1 in control and postovulatory aged oocytes (B‴). Disperse cytoplasmic distribution of NLRP5 in GV stage oocyte without prominent staining in the nucleus or surrounded nucleolus (C); enrichment of NLRP5 in the subcortical maternal complex (SCMC; arrow) beneath the oolemma in control MII oocytes (C′); loss of subcortical distribution of NLRP5 and decreased cytoplasmic staining in postovulatory-aged oocytes (C″); overall reduction in abundance of NLRP5 in control and postovulatory-aged oocytes (C‴). *U*-test: significantly different from control: ***$P < 0.001$. au, arbitrary units; OA, ovulatory ageing. Bar in A–C″: 20 µm.

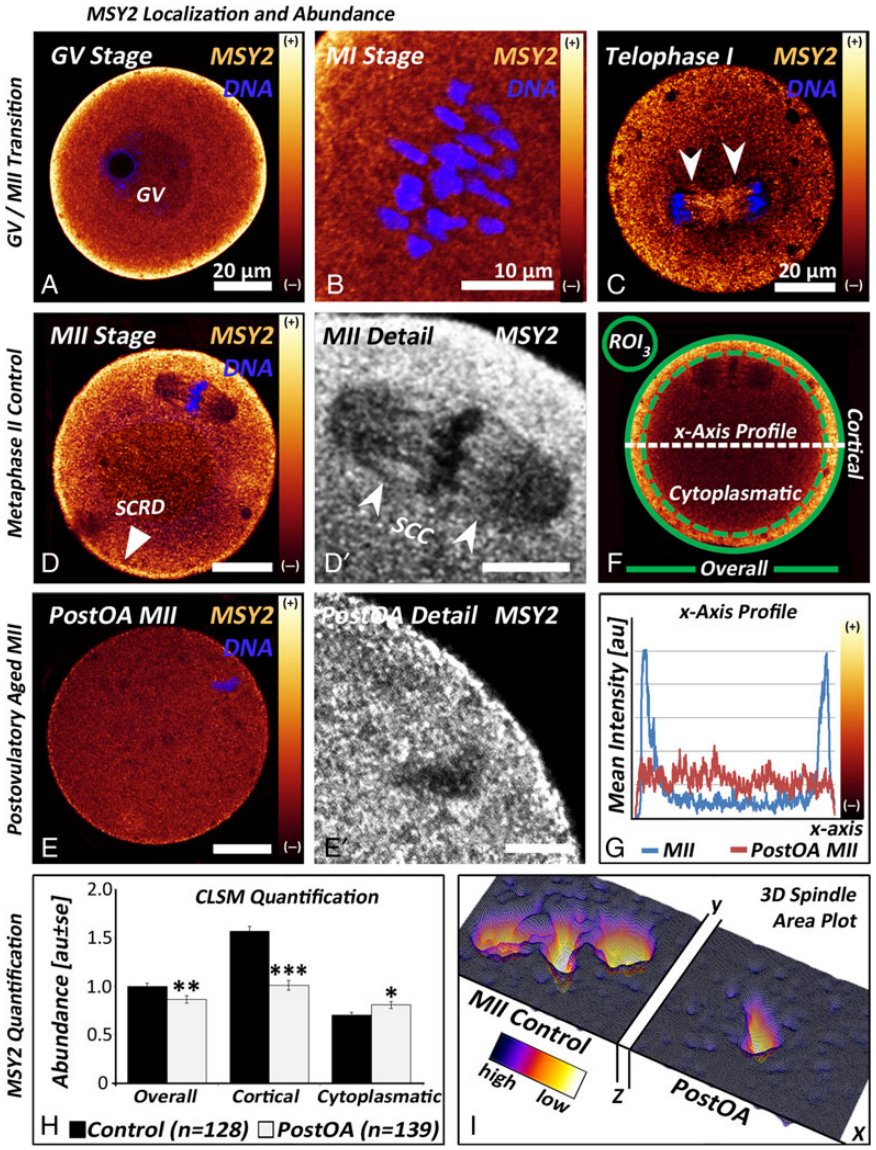

Figure 2 MSY2 localization and relative protein abundance as assessed by confocal microscopy and after exposure to nocodazole, H_2O_2 or glutathione ethyl ester (GEE). Enrichment of MSY2 in the subcortical RNP domain and in the cytosol but not in the nucleus of maturation competent germinal vesicle (GV) stage oocyte (**A**); diffuse cytoplasmic immunofluorescent staining of MSY2 in prometaphase I oocyte with still largely unaligned bivalent chromosomes (**B**); enrichment of MSY2 in the interpolar spindle, right and left to the area where cytokinesis is going to take place (arrowhead) in telophase I oocyte (**C**). Subcortical enrichment of MSY2 in the subcortical RNP domain (SCRD; arrowhead) (**D**), and enrichment in the two half spindles (D, **D′**, arrow), right and left to the well aligned chromosomes of the spindle in the control MII oocyte (D, D′). Reduced staining for MSY2 in the spindle chromosome complex (SCC) domain of postovulatory-aged oocytes (**E**) and no enrichment in the spindle of the aged oocyte (**E′**). Regions of interest (ROI) analyzed outside of the ooplasm (ROI3, background) and in the central cytoplasmic (surrounded by green dotted line) and subcortical region (defined by solid and dotted green line) for intensity of fluorescent signal for MSY2 (**F**). Cross sectional scan (white, dotted line) used for analysis of *x*-axis profile of MSY2 distribution (**F**). *x*-axis profile of relative MSY2 mean immunofluorescent intensity through the cross-section of a characteristic unaged control oocyte (blue line) and a postovulatory-aged oocyte (red line) indicating loss of cortical enrichment of MSY2 upon aging (**G**). Quantification of confocal laser scanning microscopy (CLSM) images for staining intensity in the overall cytoplasm, cortical and cytoplasmic domain of metaphase II (MII) oocytes (**H**; *u*-test: significant difference between aged and control oocytes $^*P < 0.01$: $^{**}P < 0.05$; $^{***}P < 0.001$). 3D analysis of the spindle chromosome complex (SCC)/MSY2 domain using ImageJ Surface Plot software revealing the characteristic absence (yellow color) of MSY2 at chromosomes and in the polar part of the spindle of controls (**I**, left plot), and enrichment of MSY2 in the two spindle halves between chromosomes and spindle poles (dark blue staining) of the controls; no intense staining for MSY2 at the chromosomes and only minor enrichment left and right to them in postovulatory-aged oocytes (I, right plot). MSY2 pattern in the SCC (arrowhead) of control oocytes (**J**, **J′**) and loss of MSY2 in oocytes with dispersed chromosomes exposed to nocodazole for 30 min (**K**, **K′**). Reappearance of MSY2 in the spindle (arrowhead) after recovery from nocodazole for 30 min and repolymerization of the spindle (**L**, **L′**). MSY2 abundance in control oocytes, and in oocytes aged for 2 h with or without H_2O_2 (**M**) or for 24 h in absence or presence of GEE (**N**). Significant differences: $^*P < 0.05$, $^{**}P < 0.01$ and $^{***}P < 0.001$. Bar in A, B, C, D, E, F and in J, K, L: 20 µm, in D, E′: 10 µm and in J′, K′, L′: 5 µm. Different letters in M,N indicate significant difference to *in vivo* ovulated control ($P < 0.001$).

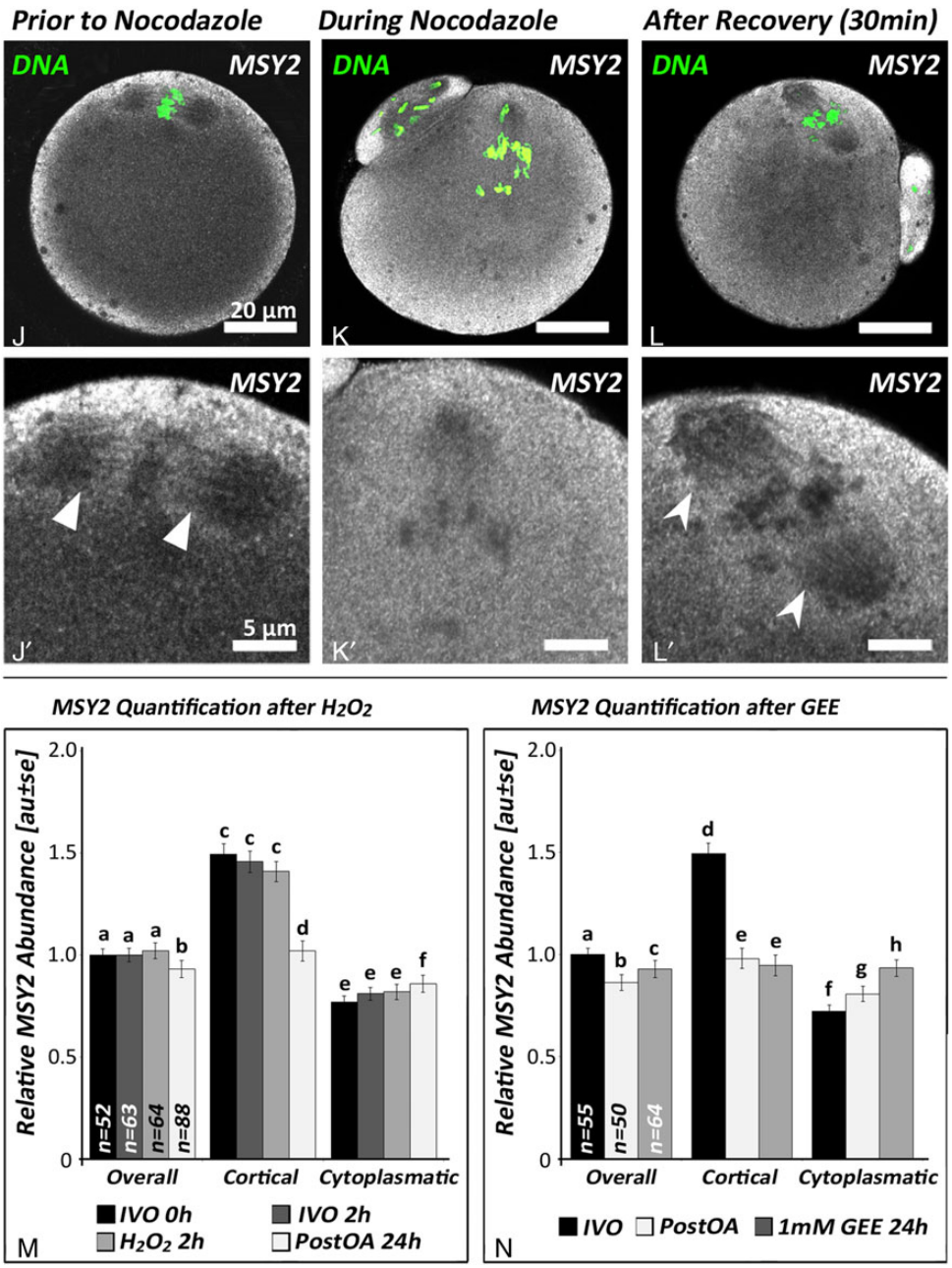

Figure 2 Continued

the SCC/MSY2 domain using ImageJ Surface Plot software (256 mesh grid size; FIRE LUT classification) confirmed characteristic MSY2 localization in a band of the two half spindles (dark magenta staining) adjacent to the area occupied by the metaphase II chromosomes that appear yellow as low staining for MSY2 (left side, Fig. 2I). Imaging showed high staining intensity, indicated by dark magenta staining in the area between chromosomes and poles and low concentrations in the central area occupied by chromosomes and the polar caps of the spindle (yellow staining) (Fig. 2I, left side, MII control). The 3D area plot of spindles of postovulatory-aged oocytes (right side of Fig. 2I; PostOA) demonstrates only little accumulation in the spindle close to chromosomes.

Semi-quantitative RT–PCR showed a 0.39 ± 0.07 times relative decrease of transcript level of *Msy2* for aged oocytes compared with controls ($P < 0.05$) (data not shown), which is in line with the decline in protein abundance. Thus, MSY2 becomes significantly altered at the transcript and the protein level and loses its typical associations with the cortex and spindle after postovulatory aging.

Spindle de-/repolymerisation causes loss and recruitment of MSY2 close to chromatin

Brief nocodazole treatment that causes spindle depolymerization leads to loss of the SCC and of MSY2 in the domain close to chromosomes

(Fig. 2K, K′) compared with controls (Fig. 2J, J′). Upon recovery the distinct MSY2 pattern in the SCC reappeared (Fig. 2L, L′), while there was no MSY2 at the flat spindle poles (arrowhead in Fig. 2L′), similar to controls (Fig. 2D′, J′).

Oxidative stress by H_2O_2 exposure does not induce immediate depletion of MSY2

H_2O_2 exposure has been used in previous studies to induce aging (di Emidio *et al.*, 2014). Increased oxidative stress by exposure of freshly ovulated MII oocytes to 10 mM H_2O_2 (Fig. 2M) did not show the same effect as postovulatory aging. Cortical or cytoplasmic level of MSY2 in the ooplasm did not change significantly compared with controls (dark bars in Fig. 2M), in contrast to postovulatory aging for 24 h (white bars in Fig. 2M).

Aging in GEE reduces age-related depletion of MSY2

The presence of 1 mM of the glutathione donor glutathione ethylester (GEE) (Fig. 2N) during aging did not prevent the dramatic loss of MSY2 from the cortical domain. However, the overall loss of MSY2 was slightly, but significantly less prominent after GEE treatment (gray bars in Fig. 2N) compared with control oocytes aged without GEE (white bars in Fig. 2N).

Protein quantification confirms reduced abundance of MSY2 and GTSF1 by aging

Western blotting showed a shift in MSY2 protein abundance and in molecular weight from ~37–39 kDa between GV and MII controls (Fig. 3A), presumably due to the phosphorylation of MSY2 by CDK1 (CDC2A) at meiotic resumption accompanied by protein degradation (Medvedev *et al.*, 2008). The MSY2 reactive bands were much fainter in MII aged oocytes (Fig. 3A, arrow), and the relative area under the curve calculation (Fig. 3B) revealed a significant decrease in MSY2 abundance after postovulatory aging.

The relative reduction in protein was confirmed by the quantitative SRM analysis (left panels, Fig. 3C) that allows the absolute quantification of proteins even in minute protein samples from oocytes and embryos (Fröhlich and Arnold, 2011; Deutsch *et al.*, 2014). Each control oocyte contains on average 0.38 fmol MSY2 protein whereas the abundance decreases significantly ($P < 0.001$) to 0.08 fmol/oocyte upon aging (Fig. 3C). Additionally, we identified selected factors involved in transcriptional control, cellular homeostasis and developmental capacity that have been detected by SRM proteomics in bovine oocytes and embryos (Deutsch *et al.*, 2014), and may be affected by aging. Absolute protein concentration was analyzed for MSY2, PDCD5, RPS27A and UHRF1, and the relative protein abundance for SMARCC1, STMN1 and GTSF1 (Table II). In contrast to MSY2, abundance of PDCD5 (Programmed cell death protein 5), RPS27A (Ubiquitin-40S ribosomal protein S27a) and UHRF1 (E3 ubiquitin-protein ligase UHRF1) (Table II) was not significantly affected by postovulatory aging (Fig. 3C and D). Total amount of PDCD5, a protein involved p53 mediated cell apoptosis and histone deacetylase 3 (Choi *et al.*, 2015; Cui *et al.*, 2015) (Table II), was ~0.3 fmol/oocyte in both, controls and also in postovulatory-aged oocytes (Fig. 3C). Protein concentration of RPS27A, a protein involved in proteasomal degradation of ubiquitinylated proteins (Wang *et al.*, 2014), was very high with an average of 11.15 fmol/oocyte in the control and 11.58 fmol/oocyte in the postovulatory aged group (Fig. 4D). Abundance of UHRF1, a multidomain protein that acts as a key element for epigenetic DNA methylation and chromatin modification (Bronner *et al.*, 2013), was also high in the control (10.51 fmol/oocyte) and slightly but not significantly altered with an average of 8.99 fmol/oocyte in the postovulatory-aged group (Fig. 3D).

Furthermore, SRM based relative quantification with crude PEPotecSRM peptides as internal standards suggests that the relative protein abundance of SMARCC1 (SWI/SNF complex subunit SMARCC1; Fig. 3E), a candidate in premature ovarian insufficiency (Norling *et al.*, 2014) and STMN1 (Stathmin; Fig. 3F) implicated in microtubule-destabilization and chromosomal instability (Holmfeldt *et al.*, 2010) was not affected by aging. However, the relative abundance of GTSF1 (Gametocyte specific factor 1), a protein that functions as a putative mRNA processing and spindle organization factor (Krotz *et al.*, 2009; Liperis *et al.*, 2013) was significantly decreased in postovulatory-aged MII oocytes with a $\log_2$-fold down-regulation of −1.7 relative to controls (Fig. 3G; $P < 0.05$).

Spindle integrity and chromosome alignment are affected by aging

Postovulatory aging can affect spindle integrity, chromosome alignment and chromatid cohesion increasing predisposition to errors in chromosome segregation (Eichenlaub-Ritter *et al.*, 1986; Dailey *et al.*, 1996; Mailhes *et al.*, 1998; Sandalinas *et al.*, 2002; Cecconi *et al.*, 2014). The majority of analyzed MII controls possessed well-aligned chromosomes at the equatorial plane and normal bi-polar spindles (Fig. 4A). Spindle abnormalities ($n = 6/73$; 8.2%) and unaligned chromosomes ($n = 8/73$; 11.0%) were rarely observed in the *in vivo* grown and matured controls (Fig. 4C). Postovulatory aging led to a significant increase in spindle abnormalities (Fig. 4B and C; $n = 46/113$; 40.7%; $P < 0.001$) and oocytes with unaligned chromosomes ($n = 55/113$; 48.7%; $P < 0.001$).

Histone H4K12 acetylation is increased while histone H3K9 trimethylation is decreased upon aging

Analysis of H4K12 acetylation pattern supports the finding of changes in histone pattern upon oocyte aging (reviewed by Ge *et al.*, 2015). There was a significant increase in H4K12 acetylation in postovulatory-aged oocytes compared with controls (control set as 1 arbitrary unit, $n = 159$; aged oocytes 1.98 arbitrary units, $n = 124$; $P < 0.01$). Analysis of trimethylation of H3K9 assessed in control (Fig. 4D–F) and in postovulatory-aged oocytes (Fig. 4E, E′) by ImageJ showed that H3K9me3 staining was reduced in aged oocytes (Fig. 4D and F). H3K9 trimethylation (Fig. 4G) decreased in parallel with increases in spindle abnormalities and unaligned chromosomes (arrows in Fig. 4E) in postovulatory-aged oocytes (Fig. 4G; $^{***}P < 0.001$).

Pericentromeric ATRX becomes increased by aging

To see if the loss of trimethylated H3K9 affects ATRX recruitment, ATRX pattern was analyzed. In GV controls, ATRX was exclusively detected within the nucleus and co-localized with chromatin (Fig. 5A), similar to previous reports (De la Fuente *et al.*, 2004). In late

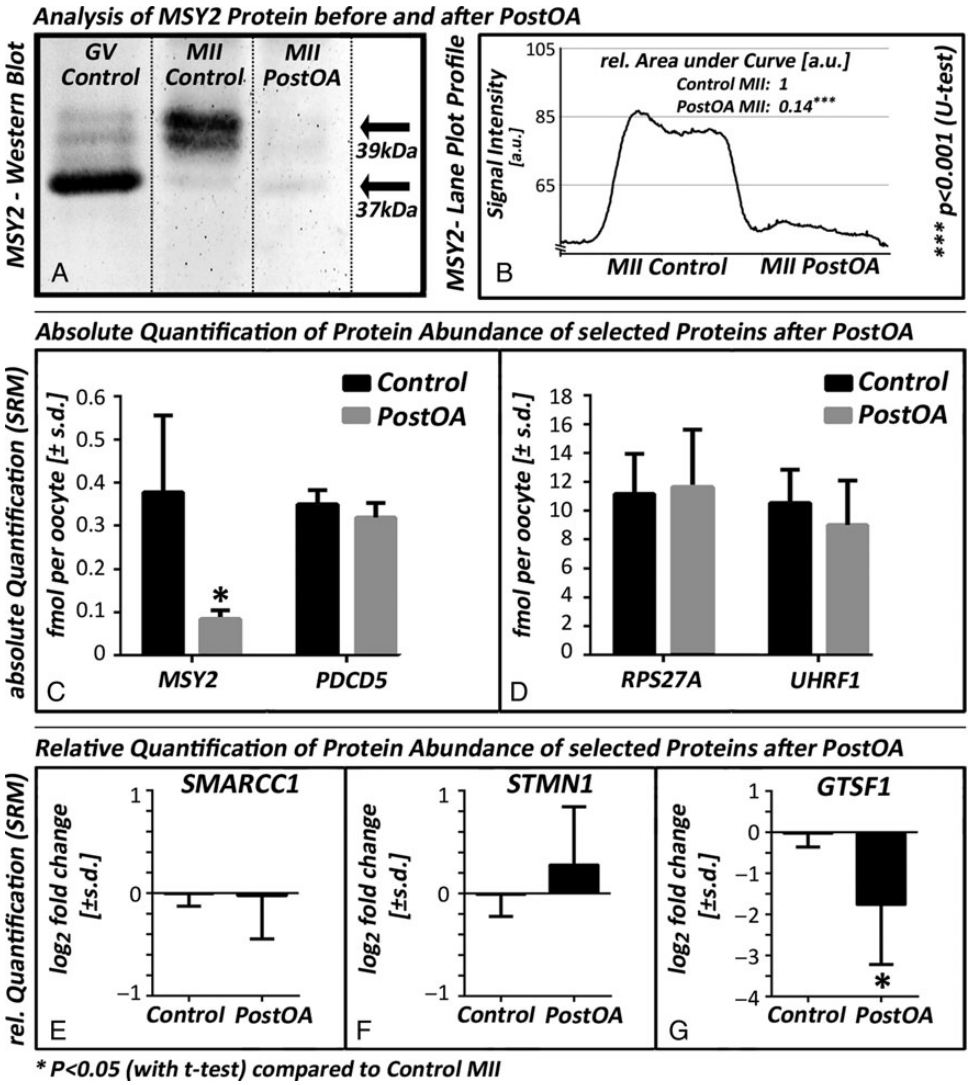

Figure 3 Absolute and relative quantification of protein abundance using western blot or selected reaction monitoring technique (SRM). Relative abundance of MSY2 protein is decreased in metaphase II (MII) controls compared with germinal vesicle (GV) stage oocytes (**A,** left and middle lane), accompanied by a shift to higher molecular weight from GV to MII of controls. Postovulatory-aged oocytes possess much less MSY2 of lower and higher MW (right panel in **A**). Lane plot profile by calculating relative area under curve using ImageJ Plot Profile software reveals significant loss of MSY2 abundance (*u*-test: ***$P < 0.001$) in postovulatory-aged MII oocytes compared with controls (**B**). Proteome analysis by selected reaction monitoring (SRM) technique with ultra pure SpikeTides TQL peptides and HeavyPeptide AQUA^{TM} Ultimate peptides reveals significant loss of MSY2 at absolute protein level (multiple *t*-test: *$P < 0.05$) after postovulatory aging but no significant abundance change in PDCD5 protein (**C**). Levels of RPS27A and UHRF1 are also not affected by aging (**D**). SRM technique and crude PEPotecSRM peptides, suggest that relative protein abundance of SMARCC1 (**E**) and STMN1 (**F**) is also not significantly altered by aging, whereas relative abundance of GTSF1 is significantly decreased (multiple *t*-test: *$P < 0.05$) in postovulatory-aged MII oocytes compared with MII controls (**G**).

prometaphase I, ATRX appeared present in distinct foci at centromeres in the pericentromeric region of homologous chromosomes (Fig. 5B). Unexpectedly, the majority of controls possessing a *Zona pellucida* with predominately well-aligned chromosomes appeared ATRX-negative or had a very weak ATRX staining ($n = 44/53$; 83.0%; Fig. 5C and inset) after conventional fixation. Only 17% (9/53) exhibited a distinct ATRX signal (Fig. 5E), similar to the percentage of oocytes with unaligned chromosomes in spindle immunofluorescence (11.0%). Contrary to expectation, 35 from 60 postovulatory aged oocytes exhibited a distinct and strong ATRX signal at the centromeres in fixed oocytes with *Zona pellucida* (Fig. 5D and E). A similar percentage of aged oocytes had particularly strong ATRX-staining (53.8%; Fig. 5E) and unaligned chromosomes (48.7%) after aging,

To test whether the increase in ATRX signal intensity is related to the activity of the spindle assembly checkpoint (SAC; reviewed in Eichenlaub-Ritter, 2012) we analyzed ATRX pattern after spindle depolymerization by the microtubule depolymerizing drug nocodazole. No or only weak ATRX signal was detected after exposure to low concentrations of nocodazole (10 μg/ml) for 10–60 min although chromosomes were often unaligned or completely scattered. Therefore,

Table II Selected proteins quantified after postovulatory ageing.

Gene symbol	Full name	Gene ID	Gene Ontology (GO) process
MSY2	Y box protein 2	MGI:1096372	mRNA stabilization Negative regulation of binding Negative regulation of translation Regulation of transcription, DNA-templated
PDCD5	Programmed cell death 5	MGI:1913538	Apoptotic process, degradation of deacetylase 3
RPS27A	Ribosomal protein S27A	MGI:1925544	Poly(A) RNA binding Translation
UHRF1	Ubiquitin-like, containing PHD and RING finger domains	MGI:1338889	Cell proliferation Maintenance of DNA methylation Chromatin modification Regulation of transcription
SMARCC1	SWI/SNF related, matrix associated, actin dependent regulator of chromatin, subfamily c, member 1	MGI:1203524	Chromatin modification Chromatin remodeling Regulation of transcription
STMN1	Stathmin 1	MGI:96739	Microtubule (de)-polymerization Mitotic spindle organization
GTSF1	Gametocyte specific factor 1	MGI:1921424	Metal ion binding Cytoskeletal organization Post-transcriptional RNA modifications
ATRX	Alpha thalassemia/mental retardation syndrome X-linked homolog	MGI:103067	Chromatin modification Transcription, DNA-templated
NLRP5	NLR family, pyrin domain containing 5	MGI:1345193	Cellular protein localization Regulation of RNA stability Regulation of protein stability *Embryonic development*
BRG1	SWI/SNF related, matrix associated, actin dependent regulator of chromatin, subfamily a, member 4	MGI:88192	DNA polymerase binding RNA polymerase II transcription co-activator Chromatin binding

postovulatory aging rather than spindle-deficiencies appear responsible for the increase of ATRX staining.

To confirm increased ATRX at centromeres, oocytes were gently spread after removal of the *Zona pellucida* (Hodges and Hunt, 2002; Vogt *et al.*, 2010; Chambon *et al.*, 2013). Spreading revealed that ATRX was present at all pericentromeres of metaphase II chromosomes in control *in vivo*-ovulated MII mouse oocytes (Fig. 5F, F′) as described (De la Fuente *et al.*, 2004; Baumann *et al.*, 2010). In addition, the much stronger signal intensity in postovulatory-aged oocytes was confirmed suggesting a major increase in ATRX at centromeres during aging (Fig. 5G, G′). ImageJ analysis (Fig. 5H) showed that average signal intensity was 8.1 a.u. in oocytes of the control ($n = 22$) and more than double in postovulatory-aged oocytes (17.9 a.u.; $n = 32$; $P < 0.001$).

Discussion

RNA and proteome homeostasis in maturation, preimplantation and aging

During oocyte growth and maturation factors are recruited, modified, expressed and stored in a stage-specific manner to ensure the highly coordinated OET (Li *et al.*, 2010; Clift and Schuh, 2013; Labrecque *et al.*, 2015). Postovulatory aging appears to interfere with these processes and thus, limits the developmental capacity (Tarín *et al.*, 1999; Liang *et al.*, 2008; Miao *et al.*, 2009; Ono *et al.*, 2011; Heinzmann *et al.*, 2015). Oxidative stress and DNA damage (Lacham-Kaplan and Trounson, 2008; Tatone *et al.*, 2011; Lord *et al.*, 2013), imbalanced redox regulation (Tarín, 1996; Tatone *et al.*, 2011), mitochondrial dysfunction, and an altered Ca^{2+} homeostasis (Tarín, 1996; Miao *et al.*, 2009; Zhang *et al.*, 2011) have all been discussed as major causes for the impaired developmental competence (Eichenlaub-Ritter, 2012), while less is known regarding the exact molecular mechanism and changes in expression. We show here that poly(A)mRNAs become significantly less abundant after aging.

Over 3500 proteins are present in metaphase II oocytes, and about 2000 in zygotes (reviewed in Yurttas *et al.* (2010), Wang *et al.* (2010) and Pfeiffer *et al.* (2011)). In addition, protein profile changes (Jiang *et al.*, 2011) were observed during postovulatory-aging in porcine oocytes, and forty-four proteins decreased by a $\log_2$-fold of about −2 from bovine MII stage to 4-cell embryos (Deutsch *et al.*, 2014) suggesting a significant degradation of maternal proteins upon activation (Wang *et al.*, 2010). In mice, postovulatory-aging leads to alterations in spindle-

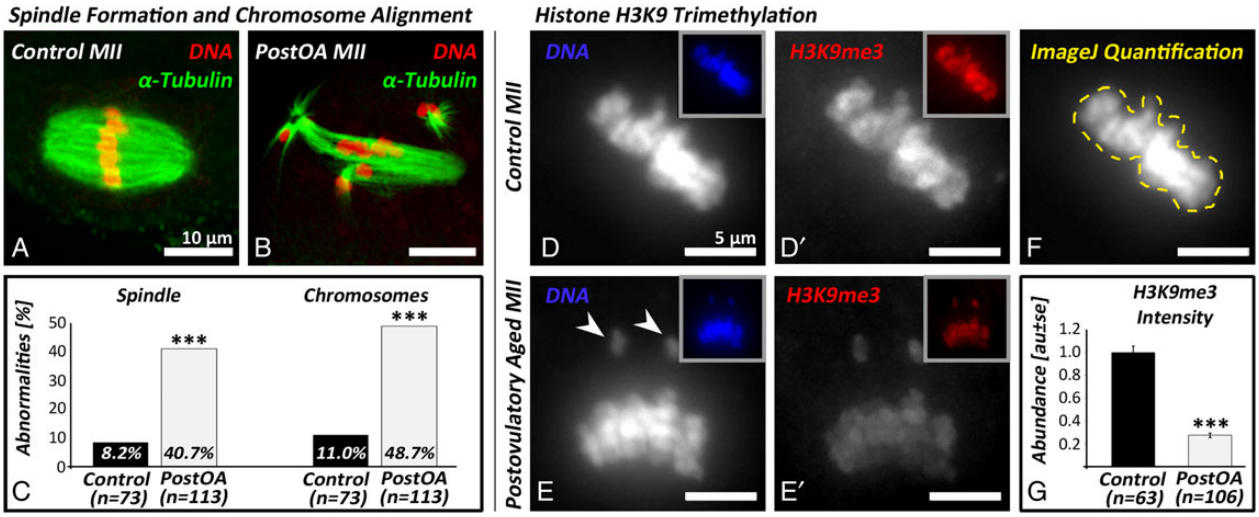

Figure 4 Characteristics of spindle morphology and chromosome alignment in control (**A**) and postovulatory-aged oocytes (**B**). Quantitative analysis reveals significant increase (***$P < 0.001$) in oocytes with spindle abnormalities (**C**, left part) and chromosome misalignment (C, right part). Semi-quantitative assessment of trimethylated H3K9 on chromosomes of control (**D**, **D′**) and postovulatory-aged (**E**, **E′**) metaphase II (MII) oocytes. Controls are characterized by well-aligned chromosomes (D) and high levels of H3K9me3 (D′), whereas postovulatory-aged oocytes often exhibit unaligned chromosomes (arrowhead in **E**) and reduced intensity of H3K9me3 fluorescence (**E′**). Semi-quantitative analysis by ImageJ software in the region of interest defined by the presence of chromosomes (**F**) reveals a significant reduction (*u*-test: ***$P < 0.001$) in chromosome-associated abundance of H3K9me3 (**G**). Bar in A, B: 10 µm, and 5 µm in D–E′.

specific proteins and reduced expression of v-akt murine thymoma viral oncogene homolog 1 (Akt) protein by 33 h post hCG, proteins that are implicated in chromosome segregation and cell survival (Cecconi *et al.*, 2014). Loss of mRNA abundance and polyadenylation of MEGs that occurs 24 h after postovulatory-aging of *in vivo*-grown murine MII oocytes (Dankert *et al.*, 2014) is shown here to be also accompanied by reduced protein abundance of several MEGs that are essential for normal development and gene expression during embryogenesis.

Transcriptome versus polyadenylation versus proteome

Loss or gain of message is not inevitably mandatory for protein abundance (Schwanhausser *et al.*, 2011; Deutsch *et al.*, 2014; Schwarzer *et al.*, 2014). Thus, especially the highly coordinated and timed recruitment of message and protein in distinct cellular compartments is crucial to ensure the cellular functionality during OET (Flemr *et al.*, 2010; Yurttas *et al.*, 2010; Chen *et al.*, 2011). Mature oocytes possess distinct cellular compartments like the subcortical maternal complex (SCMC), spindle chromosome complex (SCC) or the SCRD to store either messages or proteins (Li *et al.*, 2008; Flemr *et al.*, 2010; Romasko *et al.*, 2013; Zhu *et al.*, 2015). *In situ* hybridization with poly(dT)$_{20}$-oligonucleotides revealed now a characteristic distribution and change in abundance of poly(A)-residues at different stages of maturation (GV, MII) and after PostOA, respectively. RNA-Seq profiling provided the same picture, revealing a loss of poly(A)-mRNA at MII stage and different polyadenylation levels at GV and MII stage (Reyes *et al.*, 2015).

Individual transcripts have been studied after postovulatory aging (Tay *et al.*, 2003; Weill *et al.*, 2012; Dankert *et al.*, 2014) but not the downstream effects on the proteome. For two maternal effect genes (*Brg1* and *Nlrp5*) with reduced mRNA levels after postovulatory aging (Dankert *et al.*, 2014) the protein abundance became decreased irrespective of whether mRNAs had a similar (*Brg1*) or an altered (*Nlrp5*) poly(A)-tail length, while the specific cellular distribution was unaffected. It seems that each individual transcript exhibits a defined translational control and its fate can be defined by the requested availability of the message/protein in response for their function (Chen *et al.*, 2011; Romasko *et al.*, 2013; Gohin *et al.*, 2014).

Post-transcriptional regulation can be mediated through many factors, e.g. DAZL, an RNA-binding protein known to play a key role in germ-cell development, cytoplasmic polyadenylation elements (CPE), or U(3)GU(3) sequences that are important for mRNA recruitment. Other stage-specific transcripts do not contain such motifs (Chen *et al.*, 2011; Gohin *et al.*, 2014). *Nlrp5* that is crucial for early embryonic development (Wu, 2009; Pisani *et al.*, 2010) does not exhibit a CPE motif, but *Brg1* involved in chromatin remodeling and ZGA (Bultman *et al.*, 2006) contains one CPE motif within 150 base pairs of the polyadenylation signal motif (Dankert *et al.*, 2014). This indicates not a stringent correlation between the transcript abundance versus polyadenylation events versus proteome profile as has also been suggested by novel refined proteome analysis in bovine oocytes and zygotes (Deutsch *et al.*, 2014). Apparently, the length of the poly(A)-tail represents only a short snapshot for the stage-specific protein synthesis that is not representative for the entire translational activity during the OET. Delayed fertilization appears to interfere with intracellular mechanisms other than and in addition to polyadenylation that regulate expression prior to ZGA.

mRNA storage and availability

Long-termed storage of message depends on mRNA-binding proteins that regulate spatial-temporal accumulation, recruitment, modification

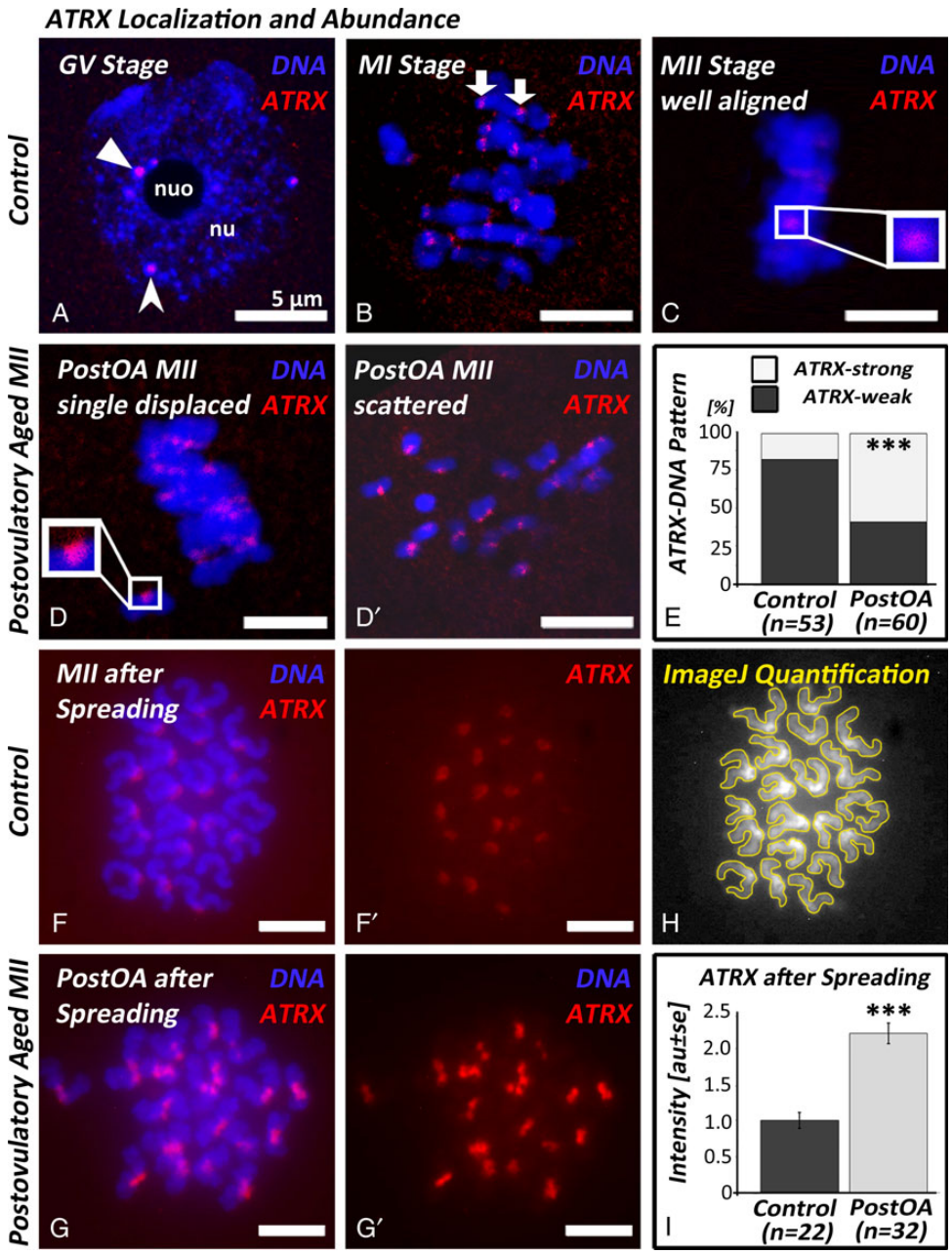

Figure 5 Localization and abundance of ATRX in control (**A**, **B**, **C**) and postovulatory-aged (**D**, **D′**), in spread control (**F**, **F′**) and postovulatory aged oocytes (**G**, **G′**) and by ImageJ quantification of area occupied by chromosomes (**H**, **I**). ATRX is observed on some (pericentromeric) heterochromatin foci in the nucleus (Nu) of germinal vesicle (GV) stage oocytes and at the rim of the nucleolus (Nuo, seen as hollow sphere) (arrow; **A**), and at the centromeres and pericentromeric chromatin of homologous chromosomes within bipolarly attached bivalents in prometaphase I/metaphase I oocytes (arrows, B), but difficult to detect on centromeres of chromosomes in mature control metaphase II oocytes (C). In postovulatory-aged oocytes ATRX appears increased at centromeres/pericentromeres of metaphase II chromosomes, irrespective of whether one (D) or most chromosomes (D′) are displaced from the spindle equator (D′). Quantification of numbers of oocytes with ATRX-strong or ATRX-weak staining reveals a significant increase (***$P < 0.001$) in the percentage of ATRX-strong staining oocytes (**E**). Presence of ATRX in pericentromeric region of all metaphase II chromosomes as evident in spread oocytes fixed after *Zona* removal (F, F′) and much more intense staining for ATRX in spread postovulatory-aged oocytes (G, G′), as also quantified by ImageJ analysis of spread oocytes (I); significant difference to controls, $P < 0.001$. Bars in A–G′: 5 µm.

and protein expression during maturation and early development (Yu *et al.*, 2001; Yang *et al.*, 2005; Medvedev *et al.*, 2008). MSY2 is a well-known mRNA binding factor that is also involved in MEG mRNA dynamics (Medvedev *et al.*, 2008, 2011; Flemr *et al.*, 2010; Ma *et al.*, 2013). As shown here MSY2 is enriched in the cortex and spindle in mature MII oocytes. In the SCRD and also in the SCC, MSY2 acts presumably for positioning selected mRNAs to ensure protein synthesis and functionality in distinct cellular compartments. Very recently, transcript analysis in

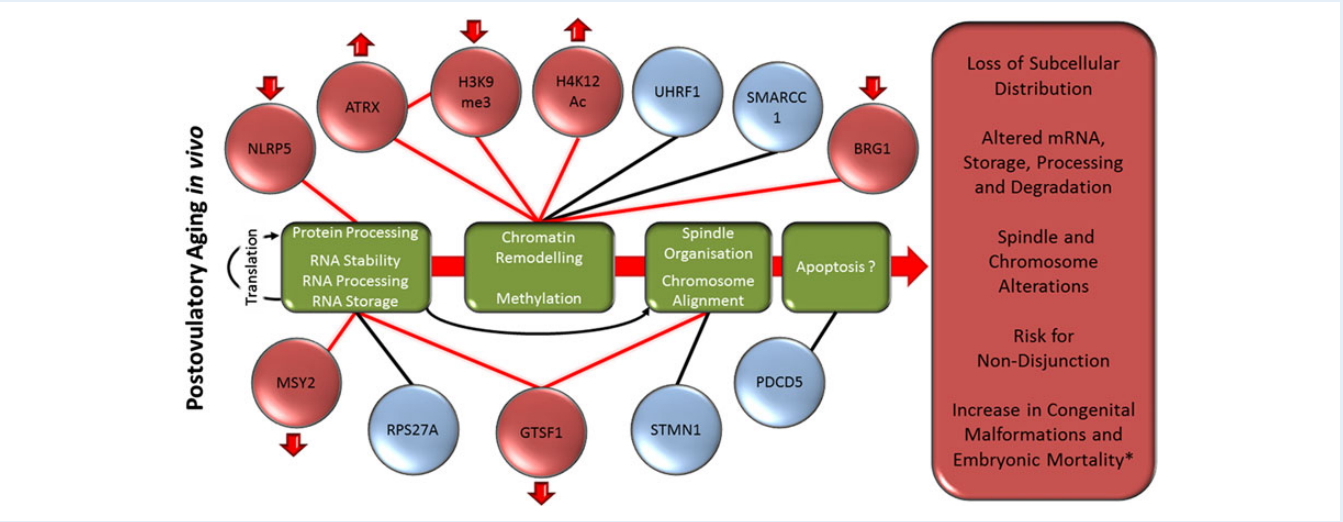

Figure 6 Pathways affected by postovulatory aging and possible consequences due to alterations in abundance of maternal effect proteins NLRP5 and BRG1, loss of MSY2 and GTSF1 protein, increased expression of ATRX, decrease in trimethlyation of H3K9, and increased H4K12 acetylation, respectively, at the pericentromeric heterochromatin with respect to transcriptome, chromatin remodeling and epigenetic status, spindle and chromosome alignment and induction of apoptosis and altered gene expression compromising oocyte quality, pre- and post-implantation development and increases in congenital abnormalities and mortality.

the SCC revealed a large subset of transcripts that are necessary for spindle formation, chromosome alignment and epigenetic modifications (e.g. *Dnmt1*, *Atrx*, *Hdac2*, *Mis18a*; Romasko *et al.*, 2013). Whether MSY2 ensures the storage of these transcripts in the spindle remains unclear, but function and distribution indicates its prominent role in SCC control and functionality.

Postovulatory aging leads to loss of MSY2 in the SCC domain and a clear translocation from the subcortical region to the cytoplasm. Apart from MSY2 only one out of six analyzed proteins quantified by SRM showed also a significantly reduced abundance. While PDCD5 (apoptotic processes), RPS27A (Poly(A) RNA binding and translation), UHRF1 (cell proliferation and maintenance of DNA methylation), SMARCC1 (chromatin modification and remodeling), STMN1 (microtubule (de)-polymerization and mitotic spindle organization) (Table II) exhibited similar protein pattern, abundance of GTSF1 was significantly reduced upon aging. Interestingly, GTSF1 is a putative factor involved in metal ion binding, cytoskeletal organization and post-transcriptional RNA modifications. Therefore, loss of GTSF1 can contribute to alterations in the translational control and also cytoskeleton integrity (Liperis *et al.*, 2013). The alterations in abundance and localization of proteins and their downstream effects are schematically depicted in Fig. 6.

MSY2 appears to have a crucial role in regulating mRNA stability, proper spindle formation and chromosome alignment. Nocodazole treatment showed that accumulation of MSY2 in the vicinity of chromosomes requires the presence of microtubules indicating a regulatory loop between cytoskeletal integrity and spatial control of translation.

CDK1-mediated phosphorylation of MSY2 leads to an irreversible protein degradation, which downstream also relies on DCP1A and DCP2 (Ma *et al.*, 2013; Mehlmann, 2013) and on mobilization of *Cnot7* mRNA that causes mRNA deadenylation (Ma *et al.*, 2015). CNOT7 activities appear also involved in reduced abundance of *Gtsf1* mRNA during mouse oocyte maturation (Ma *et al.*, 2015). Postovulatory-aging leads to reduced abundance of GTSF1 possibly by precocious mRNA release. Aging can thus initiate processing of mRNAs and proteins prior to the normal time window thereby inducing the unstoppable onset of intrinsic cellular programs that are normally activated at fertilization and early development.

Aging is more destructive than oxidative stress and may partially be prevented by GEE

In vitro maturation and postovulatory aging of mammalian oocytes are associated with loss of GSH (Hao *et al.*, 2009; Curnow *et al.*, 2010a,b), and interfere with enzymes involved in GSH-dependent pathways (Tarín *et al.*, 2004; Hendriks *et al.*, 2015). Supplementation of the antioxidant GEE reduced the loss of MSY2 during postovulatory aging. GSH is known to be involved in post-translational protein modifications, spindle formation and mitochondrial functionality (Luberda, 2005). Loss of GSH may therefore be related to mitochondrial dysfunctions, and the limited capacity to ensure proper spindle function after postovulatory aging (Tarín, 1996; Miao *et al.*, 2009; Zhang *et al.*, 2011). A recent study reported that the effects of postovulatory-aging were also reduced by N-acetyl-l-cysteine (Li and Cui, 2015). Cysteine is involved in the rate limiting step in glutathione synthesis and thus may act similar to GEE.

Oxidation by H_2O_2 was not sufficient to cause rapid loss of MSY2 in cytoplasm of MII oocytes. In contrast, GEE supplementation appears beneficial to conserve MSY2 abundance by providing sufficient reducing power to counteract the detrimental aging effect.

Spindle formation, epigenetic modifications and aging

Chromosome alignment relies on epigenetic histone and DNA modifications in oocytes. Postovulatory aging causes alterations in abundance of spindle-specific proteins and transcripts (e.g. *Mad2*) in several species (Ma *et al.*, 2005; Steuerwald *et al.*, 2005; Chen *et al.*, 2006; Lee *et al.*,

2013; Cecconi et al., 2014; Lebedeva et al., 2014) and in acetylation of α-tubulin that regulates microtubule stability and turn-over (Lee et al., 2013; Schatten and Sun, 2014). Since postovulatory aging also decreased, the reproductive fitness and longevity of the offspring in the F1 generation in mouse there may be an epigenetic component (Tarín et al., 2002). In fact, spindle alterations and chromosome misalignment are accompanied by several abnormal epigenetic histone modifications (Ge et al., 2015). For instance, acetylation of H4K12 was increased during *in vitro* aging of porcine oocytes (Cui et al., 2011). Also, histone H3K14, H4K8, H4K12 and H4K16 acetylation was altered during postovulatory aging in mice (Huang et al., 2007; Yu et al., 2007; Liang et al., 2012). SIRT1, a histone deacetylase is altered after chronological aging (Di Emidio et al., 2014), while less is known after postovulatory aging. Post-translational histone (de)-acetylation often goes along with histone methylation and *vice versa*. For instance, histone H3K9 deacetylation is followed by its trimethylation during oocyte maturation (Peters et al., 2001; Grewal and Jia, 2007; Russo et al., 2013). Insufficient H3K9 deacetylation in *in vitro*-matured human oocytes was associated with aberrant meiosis (Huang et al., 2012). Loss of H3K9 methylation was reported in chronologically aged and *in vitro* aged mouse oocytes (Yu et al., 2007; Manosalva and González, 2010). Abnormal activities of histone methyltransferases may also play a crucial role in altered epigenetic modifications in postovulatory-aged oocytes (Fig. 6). For future work it is therefore crucial to assess protein expression and activity of specific histone deacetylases and methyltransferases for instance by absolute quantification by SRM.

ATRX as indicator for fertilization-independent events during aging

ATRX is a well-known chromatin-remodeling factor that regulates epigenetic DNA and histone modifications. At metaphase II ATRX binds to pericentromeric heterochromatin where it is involved in chromosome alignment of the chromosomes (De la Fuente et al., 2004, 2012, 2015; Baumann et al., 2010). Loss of ATRX during meiosis I results in chromosome segregation defects leading to aneuploidy (De la Fuente et al., 2004, 2012, 2015; Baumann et al., 2010). ATRX is also required for the formation of a normal meiotic metaphase II spindle, centromere stability and chromosome alignment, epigenetic control of heterochromatin and DNA repair (De la Fuente et al., 2015). The majority of control MII oocytes exhibited only a relatively weak ATRX signal at the pericentromeric region when chromosomes were mainly aligned as previously reported (Baumann et al., 2010). The present data suggest that postovulatory aging induces increased expression and recruitment of ATRX to pericentromeric chromatin but also to decreased H3K9 trimethylation. This appears paradoxical as reduced rather than increased ATRX expression is linked to the deficient transcript abundance of some histone methyltransferases (De la Fuente et al., 2015). However, ATRX is strongly expressed in zygotes and it contributes to epigenetic asymmetry and repression of major satellite transcripts in the maternal genome after fertilization (De la Fuente et al., 2015). If repression occurs precociously during postovulatory aging, it can give rise to epimutations. This includes those in genomic imprinting (e.g. altered *Snrpn*; Liang et al., 2008), changes in the epigenome in placentas of delayed fertilization involving aged-oocytes (altered *H19*; Liang et al., 2011a), and epimutations in offspring from aged oocytes (altered *Peg*; Liang et al., 2011b), possibly explaining the declined H3K9me3 signal observed in the current study.

Conclusion

It appears that from onset of maturation some (unstoppable) cellular programs occur that are partially independent of fertilization. Aging can also interfere with timed spatial distribution of transcripts and proteins. However, not a global but rather a protein specific degradation of selected factors (e.g. BRG1, NLRP5, MSY2, GTSF1) is influenced by postovulatory aging. The loss of integrity of cellular compartments like the SCC or the SCMC limits several downstream cascades and the local availability of transcripts and proteins where they are normally needed. Human maternal effect NLRP7 and KHDC3L are similarly to mouse NLPR5 enriched in the cortical ooplasm (Akoury et al., 2015). Precocious loss of these factors in the SCMC (like NLRP5) could interfere with normal early embryogenesis, while alterations in the SCC-MSY2 domain and in chromatin remodeling factor BRG1 potentially disrupt proper epigenetic histone modifications (H4K12, H3K9 and H3K4 methylation) and spindle integrity (Bultman et al., 2006). Especially loss of H3K9 trimethylation, that is mandatory for normal formation of the bipolar spindle and chromosome alignment, could contribute to risks for aneuploidy.

Suboptimal environmental conditions at aging may also affect the intrinsic glutathione redox homeostasis that is crucial for mitochondrial functionality and spindle formation. This is of importance for human clinical applications, since several ART procedures interfere with the normal time window and are in an oxidative environment. Supplementation of redox scavengers like GEE to media may therefore reduce risks by *ex situ* fertilization, cryopreservation, and postovulatory aging.

Supplementary data

Supplementary data are available at http://humrep.oxfordjournals.org/.

Acknowledgements

The authors thank Ilse Betzendahl for excellent technical assistance. The study has been supported by DFG (EI 199/7-1 | GR 1138/12-1 | HO 949/21-1 and FOR 1041).

Authors' roles

T.T., M.H., D.Da., H.D., and D.De. performed data acquisition and analysis and contributed to drafting of the article. All authors, in particular, T.F., R.G., B.H. and U.E. who supervised the experimental work were involved in critical intellectual input and study design, interpretation of data, and drafting, critical revision and approval of the paper for final submission of the manuscript.

Funding

The study has been supported by the German Research Foundation (Deutsche Forschungsgemeinschaft, DFG) (EI 199/7-1 | GR 1138/12-1 | HO 949/21-1 and FOR 1041).

Conflict of interest

None declared.

References

Akoury E, Zhang L, Ao A, Slim R. NLRP7 and KHDC3L, the two maternal-effect proteins responsible for recurrent hydatidiform moles, co-localize to the oocyte cytoskeleton. *Hum Reprod* 2015;**30**:159–169.

Baumann C, Viveiros MM, De La Fuente R. Loss of maternal ATRX results in centromere instability and aneuploidy in the mammalian oocyte and pre-implantation embryo. *PLoS Genet* 2010;**6**:e1001137.

Bettegowda A, Smith GW. Mechanisms of maternal mRNA regulation: implications for mammalian early embryonic development. *Front Biosci* 2007;**2**:3713–3726.

Blandau RJ, Young WC. The effects of delayed fertilization on the development of the guinea pig ovum. *Am J Anatomy* 1939;**64**:303–329.

Bronner C, Krifa M, Mousli M. Increasing role of UHRF1 in the reading and inheritance of the epigenetic code as well as in tumorigenesis. *Biochem Pharmacol* 2013;**86**:1643–1649.

Bultman SJ, Gebuhr TC, Pan H, Svoboda P, Schultz RM, Magnuson T. Maternal BRG1 regulates zygotic genome activation in the mouse. *Genes Dev* 2006;**20**:1744–1754.

Cecconi S, Rossi G, Deldar H, Cellini V, Patacchiola F, Carta G, Macchiarelli G, Canipari R. Post-ovulatory ageing of mouse oocytes affects the distribution of specific spindle-associated proteins and Akt expression levels. *Reprod Fertil Dev* 2014;**26**:562–569.

Chambon JP, Hached K, Wassmann K. Chromosome spreads with centromere staining in mouse oocytes. *Methods Mol Biol* 2013;**957**: 203–212.

Chang MC. An experimental analysis of female sterility in the rabbit. *Fertil Steril* 1952;**3**:251–262.

Chen W, Liu Q, Li Z, Wang XR, Zhu GJ. Influence of postovulatory ageing on balanced predivision of sister chromatid in mouse oocytes. *Zhonghua Yi Xue Yi Chuan Xue Za Zhi* 2006;**23**:256–259.

Chen J, Melton C, Suh N, Oh JS, Horner K, Xie F, Sette C, Blelloch R, Conti M. Genome-wide analysis of translation reveals a critical role for deleted in azoospermia-like (Dazl) at the oocyte-to-zygote transition. *Genes Dev* 2011;**25**:755–766.

Choi HK, Choi Y, Park ES, Park SY, Lee SH, Seo J, Jeong MH, Jeong JW, Jeong JH, Lee PC *et al.* Programmed cell death 5 mediates HDAC3 decay to promote genotoxic stress response. *Nat Commun* 2015; **6**:7390.

Clift D, Schuh M. Restarting life: fertilization and the transition from meiosis to mitosis. *Nat Rev Mol Cell Biol* 2013;**14**:549–562.

Cui MS, Wang XL, Tang DW, Zhang J, Liu Y, Zeng SM. Acetylation of H4K12 in porcine oocytes during in vitro aging: potential role of ooplasmic reactive oxygen species. *Theriogenology* 2011;**75**:638–646.

Cui X, Choi HK, Choi YS, Park SY, Sung GJ, Lee YH, Lee J, Jun WJ, Kim K, Choi KC *et al.* DNAJB1 destabilizes PDCD5 to suppress p53-mediated apoptosis. *Cancer Lett* 2015;**357**:307–315.

Curnow EC, Ryan JP, Saunders DM, Hayes ES. Oocyte glutathione and fertilisation outcome of Macaca nemestrina and Macaca fascicularis in in vivo- and in vitro-matured oocytes. *Reprod Fertil Dev* 2010a;**22**:1032–1040.

Curnow EC, Ryan JP, Saunders DM, Hayes ES. In vitro developmental potential of macaque oocytes, derived from unstimulated ovaries, following maturation in the presence of glutathione ethyl ester. *Hum Reprod* 2010b;**25**:2465–2474.

Dailey T, Dale B, Cohen J, Munné S. Association between nondisjunction and maternal age in meiosis-II human oocytes. *Am J Hum Genet* 1996; **59**:176–184.

Dankert D, Demond H, Trapphoff T, Heiligentag M, Rademacher K, Eichenlaub-Ritter U, Horsthemke B, Grümmer R. Pre- and postovulatory aging of murine oocytes affect the transcript level and poly(A) tail length of maternal effect genes. *PLoS One* 2014;**9**:e108907.

De La Fuente R, Viveiros MM, Wigglesworth K, Eppig JJ. ATRX, a member of the SNF2 family of helicase/ATPases, is required for chromosome alignment and meiotic spindle organization in metaphase II stage mouse oocytes. *Dev Biol* 2004;**272**:1–14.

De La Fuente R, Baumann C, Viveiros MM. Chromatin structure and ATRX function in mouse oocytes. *Results Probl Cell Differ* 2012;**55**:45–68.

De La Fuente R, Baumann C, Viveiros MM. ATRX contributes to epigenetic asymmetry and silencing of major satellite transcripts in the maternal genome of the mouse embryo. *Development* 2015;**142**:1806–1817.

Demant M, Trapphoff T, Fröhlich T, Arnold GJ, Eichenlaub-Ritter U. Vitrification at the pre-antral stage transiently alters inner mitochondrial membrane potential but proteome of in vitro grown and matured mouse oocytes appears unaffected. *Hum Reprod* 2012;**27**:1096–1111.

Deutsch DR, Fröhlich T, Otte KA, Beck A, Habermann FA, Wolf E, Arnold GJ. Stage-specific proteome signatures in early bovine embryo development. *J Proteome Res* 2014;**13**:4363–4376.

Di Emidio G, Falone S, Vitti M, D'Alessandro AM, Vento M, Di Pietro C, Amicarelli F, Tatone C. SIRT1 signalling protects mouse oocytes against oxidative stress and is deregulated during aging. *Hum Reprod* 2014; **29**:2006–2017.

Eichenlaub-Ritter U. Oocyte ageing and its cellular basis. *Int J Dev Biol* 2012; **56**:841–852.

Eichenlaub-Ritter U, Chandley AC, Gosden RG. Alterations to the microtubular cytoskeleton and increased disorder of chromosome alignment in spontaneously ovulated mouse oocytes aged in vivo: an immunofluorescence study. *Chromosoma* 1986;**94**:337–345.

Fair T. Mammalian oocyte development: checkpoints for competence. *Reprod Fertil Dev* 2010;**22**:13–20.

Flemr M, Ma J, Schultz RM, Svoboda P. P-body loss is concomitant with formation of a messenger RNA storage domain in mouse oocytes. *Biol Reprod* 2010;**82**:1008–1017.

Fröhlich T, Arnold GJ. Quantifying attomole amounts of proteins from complex samples by nano-LC and selected reaction monitoring. *Methods Mol Biol* 2011;**790**:141–164.

Ge ZJ, Schatten H, Zhang CL, Sun QY. Oocyte ageing and epigenetics. *Reproduction* 2015;**149**:103–114.

Gohin M, Fournier E, Dufort I, Sirard MA. Discovery, identification and sequence analysis of RNAs selected for very short or long poly A tail in immature bovine oocytes. *Mol Hum Reprod* 2014;**20**:127–138.

Grewal S, Jia S. Heterochromatin revisited. *Nat Rev Genet* 2007;**8**:835–846.

Hao ZD, Liu S, Wu Y, Wan PC, Cui MS, Chen H, Zeng SM. Abnormal changes in mitochondria, lipid droplets, ATP and glutathione content, and Ca(2+) release after electro-activation contribute to poor developmental competence of porcine oocyte during in vitro ageing. *Reprod Fertil Dev* 2009;**21**:323–332.

Heinzmann J, Mattern F, Aldag P, Bernal-Ulloa SM, Schneider T, Haaf T, Niemann H. Extended in vitro maturation affects gene expression and DNA methylation in bovine oocytes. *Mol Hum Reprod* 2015;**21**:770–782.

Hendriks WK, Colleoni S, Galli C, Paris DB, Colenbrander B, Roelen BA, Stout TA. Maternal age and in vitro culture affect mitochondrial number and function in equine oocytes and embryos. *Reprod Fertil Dev* 2015. doi: 10.1071/RD14450. (epub ahead of print).

Hodges CA, Hunt PA. Simultaneous analysis of chromosomes and chromosome-associated proteins in mammalian oocytes and embryos. *Chromosoma* 2002;**111**:165–169.

Holmfeldt P, Sellin ME, Gullberg M. Upregulated Op18/stathmin activity causes chromosomal instability through a mechanism that evades the spindle assembly checkpoint. *Exp Cell Res* 2010;**316**:2017–2026.

Huang JC, Yan LY, Lei ZL, Miao YL, Shi LH, Yang JW, Wang Q, Ouyang YC, Sun QY, Chen DY. Changes in histone acetylation during postovulatory aging of mouse oocyte. *Biol Reprod* 2007;**77**:666–670.

Huang J, Li T, Ding CH, Brosens J, Zhou CQ, Wang HH, Xu YW. Insufficient histone-3 lysine-9 deacetylation in human oocytes matured in vitro is associated with aberrant meiosis. *Fertil Steril* 2012;**97**:178–184.

Jiang GJ, Wang K, Miao DQ, Guo L, Hou Y, Schatten H, Sun QY. Protein profile changes during porcine oocyte aging and effects of caffeine on protein expression patterns. *PLoS One* 2011;**6**:e28996.

Kim KH, Lee KA. Maternal effect genes: findings and effects on mouse embryo development. *Clin Exp Reprod Med* 2014;**41**:47–61.

Kosubek A, Klein-Hitpass L, Rademacher K, Horsthemke B, Ryffel GU. Aging of Xenopus tropicalis eggs leads to deadenylation of a specific set of maternal mRNAs and loss of developmental potential. *PLoS One* 2010;**5**:e13532.

Krotz SP, Ballow DJ, Choi Y, Rajkovic A. Expression and localization of the novel and highly conserved gametocyte-specific factor 1 during oogenesis and spermatogenesis. *Fertil Steril* 2009;**91**:2020–2024.

Labrecque R, Lodde V, Dieci C, Tessaro I, Luciano AM, Sirard MA. Chromatin remodelling and histone m RNA accumulation in bovine germinal vesicle oocytes. *Mol Reprod Dev* 2015;**82**:450–462.

Lacham-Kaplan O, Trounson A. Reduced developmental competence of immature, in-vitro matured and postovulatory aged mouse oocytes following IVF and ICSI. *Reprod Biol Endocrinol* 2008;**6**:58.

Lebedeva II, Singina GN, Lopukhov AV, Zinov'eva NA. Dynamics of morphofunctional changes in aging bovine ova during the prolonged culture in vitro. *Tsitologiia* 2014;**56**:57–66.

Lee AR, Kishigami S, Amano T, Matsumoto K, Wakayama T, Hosoi Y. Nicotinamide: a class III HDACi delays in vitro aging of mouse oocytes. *J Reprod Dev* 2013;**59**:238–244.

Li Q, Cui LB. Combined inhibitory effects of low temperature and N-acetyl-l-cysteine on the postovulatory aging of mouse oocytes. *Zygote* 2015;1–11. doi:10.1017/S0967199415000039. (epub ahead of print).

Li L, Baibakov B, Dean J. A subcortical maternal complex essential for preimplantation mouse embryogenesis. *Dev Cell* 2008;**15**:416–425.

Li L, Zheng P, Dean J. Maternal control of early mouse development. *Development* 2010;**137**:859–870.

Liang XW, Zhu JQ, Miao YL, Liu JH, Wei L, Lu SS, Hou Y, Schatten H, Lu KH, Sun QY. Loss of methylation imprint of Snrpn in postovulatory aging mouse oocyte. *Biochem Biophys Res Commun* 2008;**371**:16–21.

Liang XW, Ge ZJ, Wei L, Guo L, Han ZM, Schatten H, Sun QY. The effects of postovulatory aging of mouse oocytes on methylation and expression of imprinted genes at mid-term gestation. *Mol Hum Reprod* 2011a;**17**:562–567.

Liang XW, Ge ZJ, Guo L, Luo SM, Han ZM, Schatten H, Sun QY. Effect of postovulatory oocyte aging on DNA methylation imprinting acquisition in offspring oocytes. *Fertil Steril* 2011b;**96**:1479–1484.

Liang X, Ma J, Schatten H, Sun Q. Epigenetic changes associated with oocyte aging. *Sci China Life Sci* 2012;**55**:670–676.

Liperis G, Iles D, Lu J, Cotterill M, Huntriss J, Picton H. The function of Gametocyte Specific Factor 1 (GTSF1) during ovine oocyte maturation. *Society for Reproduction and Fertility* 2013. Abstract O027.

Lord T, Nixon B, Jones KT, Aitken RJ. Melatonin prevents postovulatory oocyte aging in the mouse and extends the window for optimal fertilization in vitro. *Biol Reprod* 2013;**88**:67.

Luberda Z. The role of glutathione in mammalian gametes. *Reprod Biol* 2005;**5**:5–17.

Ma W, Zhang D, Hou Y, Li YH, Sun QY, Sun XF, Wang WH. Reduced expression of MAD2, BCL2, and MAP kinase activity in pig oocytes after in vitro aging are associated with defects in sister chromatid segregation during meiosis II and embryo fragmentation after activation. *Biol Reprod* 2005;**72**:373–383.

Ma J, Flemr M, Strnad H, Svoboda P, Schultz RM. Maternally recruited DCP1A and DCP2 contribute to messenger RNA degradation during oocyte maturation and genome activation in mouse. *Biol Reprod* 2013;**88**:11.

Ma J, Fukuda Y, Schultz RM. Mobilization of dormant Cnot7 mRNA promotes deadenylation of maternal transcripts during mouse oocyte maturation. *Biol Reprod* 2015. pii: biolreprod.115.130344.

Mailhes JB1, Young D, London SN. Postovulatory ageing of mouse oocytes in vivo and premature centromere separation and aneuploidy. *Biol Reprod* 1998;**58**:1206–1210.

Manosalva I, González A. Aging changes the chromatin configuration and histone methylation of mouse oocytes at germinal vesicle stage. *Theriogenology* 2010;**74**:1539–1547.

Medvedev S, Yang J, Hecht NB, Schultz RM. CDC2A (CDK1)-mediated phosphorylation of MSY2 triggers maternal mRNA degradation during mouse oocyte maturation. *Dev Biol* 2008;**321**:205–215.

Medvedev S, Pan H, Schultz RM. Absence of MSY2 in mouse oocytes perturbs oocyte growth and maturation, RNA stability, and the transcriptome. *Biol Reprod* 2011;**85**:575–583.

Mehlmann LM. Losing mom's message: requirement for DCP1A and DCP2 in the degradation of maternal transcripts during oocyte maturation. *Biol Reprod* 2013;**88**:10.

Messerschmidt DM, de Vries W, Ito M, Solter D, Ferguson-Smith A, Knowles BB. Trim28 is required for epigenetic stability during mouse oocyte to embryo transition. *Science* 2012;**335**:1499–1502.

Miao YL, Kikuchi K, Sun QY, Schatten H. Oocyte aging: cellular and molecular changes, developmental potential and reversal possibility. *Hum Reprod Update* 2009;**15**:573–585.

Muramatsu D, Singh PB, Kimura H, Tachibana M, Shinkai Y. Pericentric heterochromatin generated by HP1 protein interaction-defective histone methyltransferase Suv39h1. *J Biol Chem* 2013;**288**:25285–25296.

Norbury CJ. Cytoplasmic RNA: a case of the tail wagging the dog. *Nat Rev Mol Cell Biol* 2013;**14**:643–653.

Norling A, Hirschberg AL, Rodriguez-Wallberg KA, Iwarsson E, Wedell A, Barbaro M. Identification of a duplication within the GDF9 gene and novel candidate genes for primary ovarian insufficiency (POI) by a customized high-resolution array comparative genomic hybridization platform. *Hum Reprod* 2014;**29**:1818–1827.

Ohsugi M1, Zheng P, Baibakov B, Li L, Dean J. Maternally derived FILIA-MATER complex localizes asymmetrically in cleavage-stage mouse embryos. *Development* 2008;**135**:259–269.

Ono T, Mizutani E, Li C, Yamagata K, Wakayama T. Offspring from intracytoplasmic sperm injection of aged mouse oocytes treated with caffeine or MG132. *Genesis* 2011;**49**:460–471.

Peters AH, O'Carroll D, Scherthan H, Mechtler K, Sauer S, Schöfer C, Weipoltshammer K, Pagani M, Lachner M, Kohlmaier A *et al.* Loss of the Suv39h histone methyltransferases impairs mammalian heterochromatin and genome stability. *Cell* 2001;**107**:323–337.

Pfeiffer MJ, Siatkowski M, Paudel Y, Balbach ST, Baeumer N, Crosetto N, Drexler HC, Fuellen G, Boiani M. Proteomic analysis of mouse oocytes reveals 28 candidate factors of the 'reprogrammome'. *J Proteome Res* 2011;**10**:2140–2153.

Pisani LF, Ramelli P, Lazzari B, Braglia S, Ceciliani F, Mariani P. Characterization of maternal antigen that embryos require (MATER/NLRP5) gene and protein in pig somatic tissues and germ cells. *J Reprod Dev* 2010;**56**:41–48.

Reyes JM, Chitwood JL, Ross PJ. RNA-Seq profiling of single bovine oocyte transcript abundance and its modulation by cytoplasmic polyadenylation. *Mol Reprod Dev* 2015;**82**:103–114.

Romasko EJ, Amarnath D, Midic U, Latham KE. Association of maternal mRNA and phosphorylated EIF4EBP1 variants with the spindle in mouse oocytes: localized translational control supporting female meiosis in mammals. *Genetics* 2013;**195**:349–358.

Russo V, Bernabò N, Di Giacinto O, Martelli A, Mauro A, Berardinelli P, Curini V, Nardinocchi D, Mattioli M, Barboni B. H3K9 trimethylation

precedes DNA methylation during sheep oogenesis: HDAC1, SUV39H1, G9a, HP1, and Dnmts are involved in these epigenetic events. *J Histochem Cytochem* 2013;**61**:75–89.

Sandalinas M, Márquez C, Munné S. Spectral karyotyping of fresh, non-inseminated oocytes. *Mol Hum Reprod* 2002;**8**:580–585.

Schatten H, Sun QY. Posttranslationally modified tubulins and other cytoskeletal proteins: their role in gametogenesis, oocyte maturation, fertilization and Pre-implantation embryo development. *Adv Exp Med Biol* 2014;**759**:57–87.

Schwanhausser B, Busse D, Li N, Dittmar G, Schuchhardt J, Wolf J, Chen W, Selbach M. Global quantification of mammalian gene expression control. *Nature* 2011;**473**:337–342.

Schwarzer C, Siatkowski M, Pfeiffer MJ, Baeumer N, Drexler HC, Wang B, Fuellen G, Boiani M. Maternal age effect on mouse oocytes: new biological insight from proteomic analysis. *Reproduction* 2014;**148**:55–72.

Sidler C, Li D, Wang B, Kovalchuk I, Kovalchuk O. SUV39H1 downregulation induces deheterochromatinization of satellite regions and senescence after exposure to ionizing radiation. *Front Genet* 2014;**5**:411.

Steuerwald NM, Steuerwald MD, Mailhes JB. Post-ovulatory aging of mouse oocytes leads to decreased MAD2 transcripts and increased frequencies of premature centromere separation and anaphase. *Mol Hum Reprod* 2005;**11**:623–630.

Su YQ, Sugiura K, Woo Y, Wigglesworth K, Kamdar S, Affourtit J, Eppig JJ. Selective degradation of transcripts during meiotic maturation of mouse oocytes. *Dev Biol* 2007;**302**:104–117.

Takahashi T, Igarashi H, Amita M, Hara S, Matsuo K, Kurachi H. Molecular mechanism of poor embryo development in postovulatory aged oocytes: mini review. *J Obstet Gynaecol Res* 2013;**39**:1431–1439.

Tarín JJ. Potential effects of age-associated oxidative stress on mammalian oocytes/embryos. *Mol Hum Reprod* 1996;**2**:717–724.

Tarín JJ, Pérez-Albalá S, Aguilar A, Miñarro J, Hermenegildo C, Cano A. Long-term effects of postovulatory aging of mouse oocytes on offspring: a two-generational study. *Biol Reprod* 1999;**61**:1347–1355.

Tarín JJ, Pérez-Albalá S, Pérez-Hoyos S, Cano A. Postovulatory aging of oocytes decreases reproductive fitness and longevity of offspring. *Biol Reprod* 2002;**66**:495–499.

Tarín JJ, Gómez-Piquer V, Pertusa JF, Hermenegildo C, Cano A. Association of female aging with decreased parthenogenetic activation, raised MPF, and MAPKs activities and reduced levels of glutathione S-transferases activity and thiols in mouse oocytes. *Mol Reprod Dev* 2004;**69**:402–410.

Tatone C, Di Emidio G, Barbaro R, Vento M, Ciriminna R, Artini PG. Effects of reproductive aging and postovulatory aging on the maintenance of biological competence after oocyte vitrification: insights from the mouse model. *Theriogenology* 2011;**76**:864–873.

Tay J, Hodgman R, Sarkissian M, Richter JD. Regulated CPEB phosphorylation during meiotic progression suggests a mechanism for temporal control of maternal mRNA translation. *Genes Dev* 2003;**17**:1457–1462.

Trapphoff T, El Hajj N, Zechner U, Haaf T, Eichenlaub-Ritter U. DNA integrity, growth pattern, spindle formation, chromosomal constitution and imprinting patterns of mouse oocytes from vitrified pre-antral follicles. *Hum Reprod* 2010;**25**:3025–3042.

Trapphoff T, Heiligentag M, El Hajj N, Haaf T, Eichenlaub-Ritter U. Chronic exposure to a low concentration of bisphenol A during follicle culture affects the epigenetic status of germinal vesicles and metaphase II oocytes. *Fertil Steril* 2013;**100**:1758–1767.

Van den Berg IM, Eleveld C, van der Hoeven M, Birnie E, Steegers EA, Galjaard RJ, Laven JS, van Doorninck JH. Defective deacetylation of histone 4 K12 in human oocytes is associated with advanced maternal age and chromosome misalignment. *Hum Reprod* 2011;**26**:1181–1190.

Vogt E, Sanhaji M, Klein W, Seidel T, Wordeman L, Eichenlaub-Ritter U. MCAK is present at centromeres, midspindle and chiasmata and involved in silencing of the spindle assembly checkpoint in mammalian oocytes. *Mol Hum Reprod* 2010;**16**:665–684.

Wang S, Kou Z, Jing Z, Zhang Y, Guo X, Dong M, Wilmut I, Gao S. Proteome of mouse oocytes at different developmental stages. *Proc Natl Acad Sci USA* 2010;**107**:17639–17644.

Wang H, Yu J, Zhang L, Xiong Y, Chen S, Xing H, Tian Z, Tang K, Wei H, Rao Q *et al*. RPS27a promotes proliferation, regulates cell cycle progression and inhibits apoptosis of leukemia cells. *Biochem Biophys Res Commun* 2014;**446**:1204–1210.

Weill L, Belloc E, Bava FA, Mendez R. Translational control by changes in poly(A) tail length: recycling mRNAs. *Nat Struct Mol Biol* 2012;**19**:577–585.

Wu X. Maternal depletion of NLRP5 blocks early embryogenesis in rhesus macaque monkeys (Macaca mulatta). *Hum Reprod* 2009;**24**:415–424.

Yan L, Yang M, Guo H, Yang L, Wu J, Li R, Liu P, Lian Y, Zheng X, Yan J *et al.* Single-cell RNA-Seq profiling of human preimplantation embryos and embryonic stem cells. *Nat Struct Mol Biol* 2013;**20**:1131–1139.

Yang J, Medvedev S, Yu J, Tang LC, Agno JE, Matzuk MM, Schultz RM, Hecht NB. Absence of the DNA-/RNA-binding protein MSY2 results in male and female infertility. *Proc Natl Acad Sci USA* 2005;**102**:5755–5760.

Yu J, Hecht NB, Schultz RM. Expression of MSY2 in mouse oocytes and preimplantation embryos. *Biol Reprod* 2001;**65**:1260–1270.

Yu JN, Wang M, Wang DQ, Li SH, Shao GB, Wu CF, Liu HL. Chromosome changes of aged oocytes after ovulation. *Yi Chuan* 2007;**29**:225–229.

Yurttas P, Morency E, Coonrod SA. Use of proteomics to identify highly abundant maternal factors that drive the egg-to-embryo transition. *Reproduction* 2010;**139**:809–823.

Zhang K, Smith GW. Maternal control of early embryogenesis in mammals. *Reprod Fertil Dev* 2015. doi:10.1071/RD14441. (epub ahead of print).

Zhang N, Wakai T, Fissore RA. Caffeine alleviates the deterioration of Ca(2+) release mechanisms and fragmentation of in vitro-aged mouse eggs. *Mol Reprod Dev* 2011;**78**:684–701.

Zhu K, Yan L, Zhang X, Lu X, Wang T, Yan J, Liu X, Qiao J, Li L. Identification of a human subcortical maternal complex. *Mol Hum Reprod* 2015; **21**:320–329.

Zuccotti M, Merico V, Cecconi S, Redi CA, Garagna S. What does it take to make a developmentally competent mammalian egg? *Hum Reprod Update* 2011;**17**:525–540.